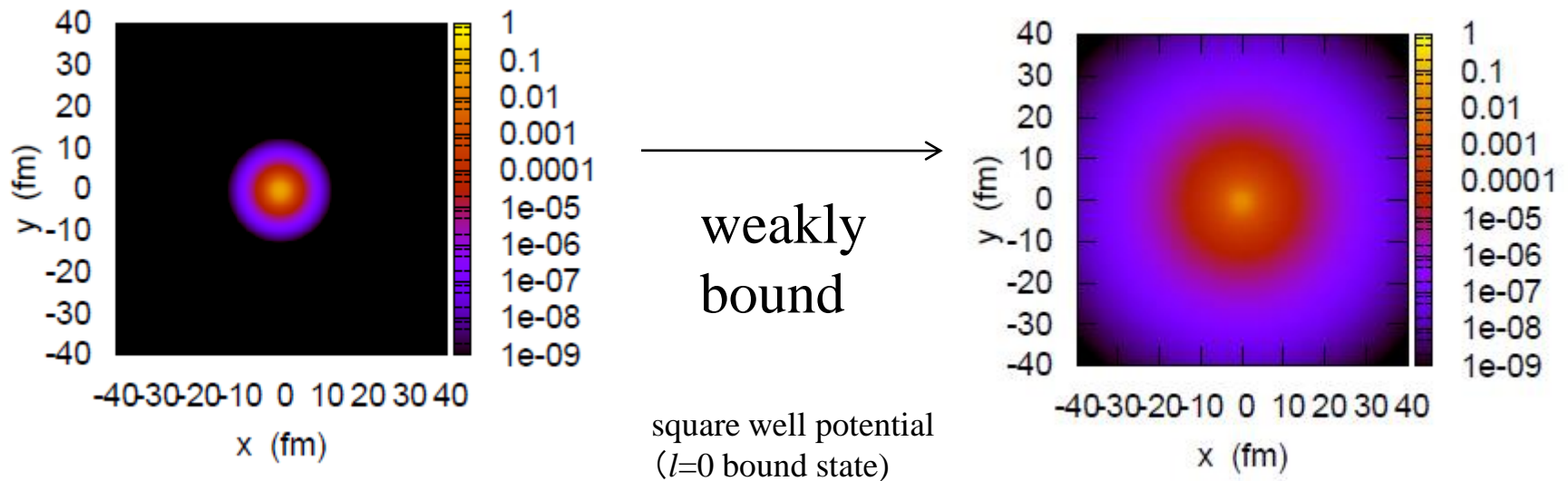
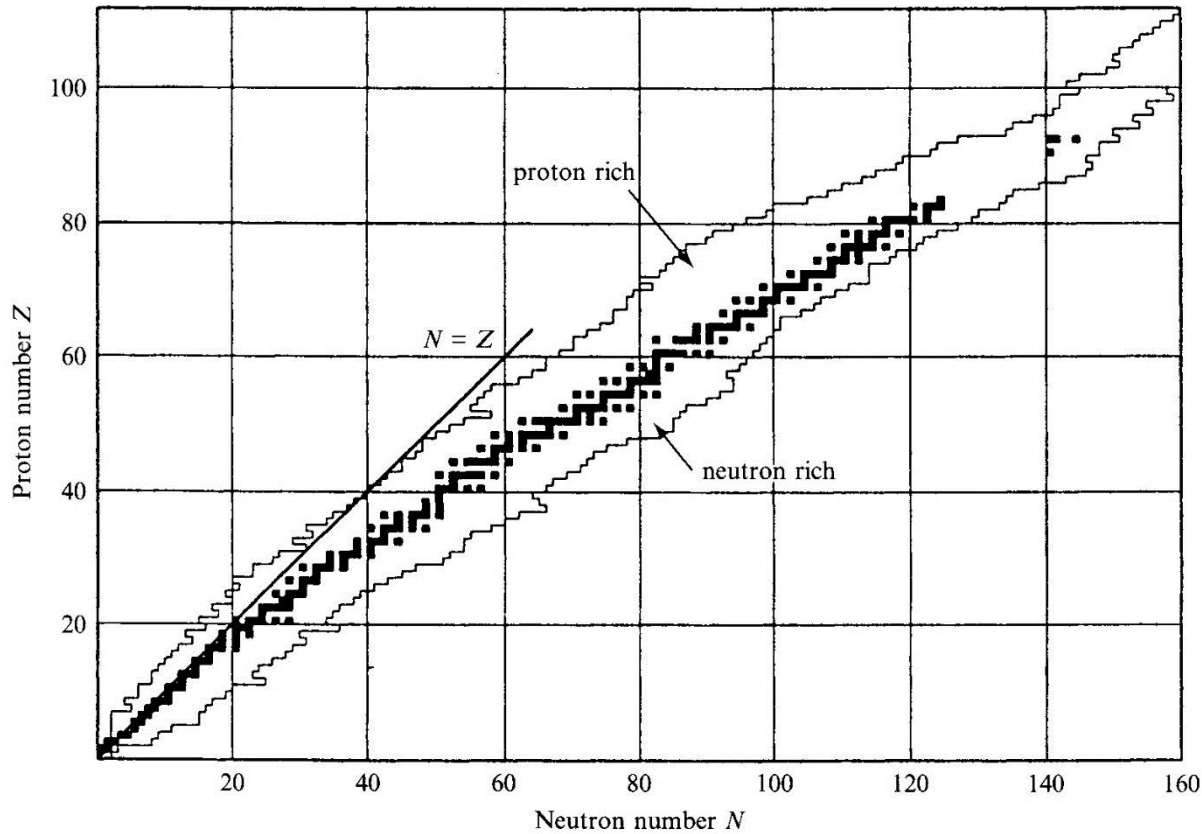


Properties of one-neutron halo nuclei

- bound states
- Effects of angular momentum
- Coulomb excitations
- Deformation



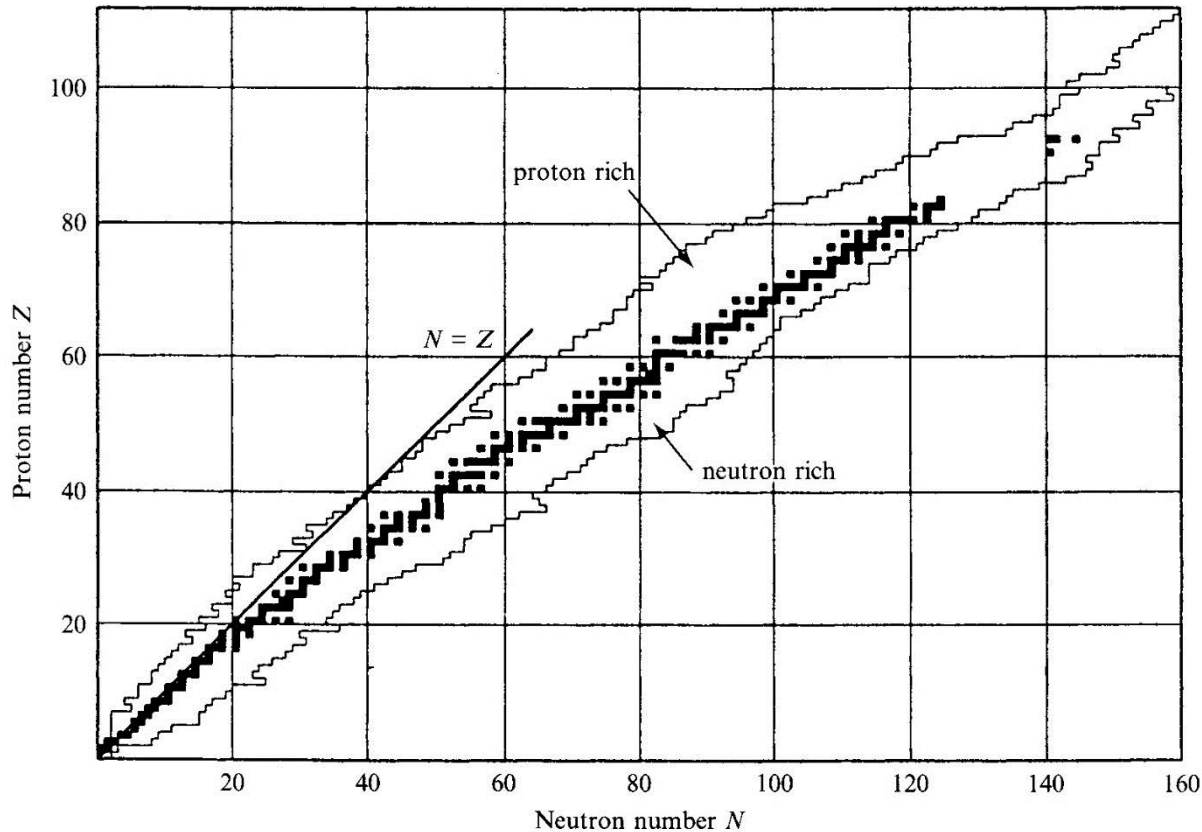
Nuclear Chart



Nuclear Physics: developed for stable nuclei (until mid 1980's)

saturation, radii, binding energy,
magic numbers and independent particle....

Nuclear Chart

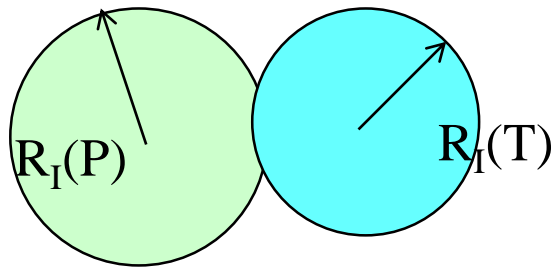
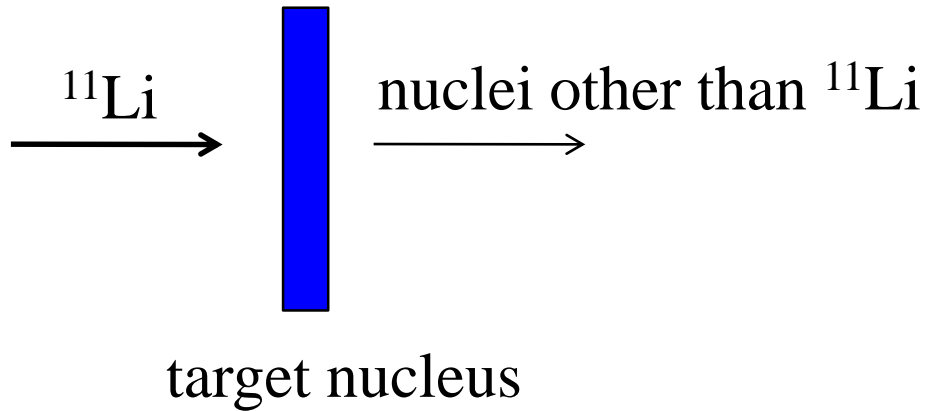


Nuclear Physics: developed for stable nuclei (until mid 1980's)

natural questions:

- how many neutrons can be put into a nucleus when the number of proton is fixed?
- what are the properties of nuclei far from the stability line?

Start of a research on unstable nuclei: interaction cross sections (1985)



projectile

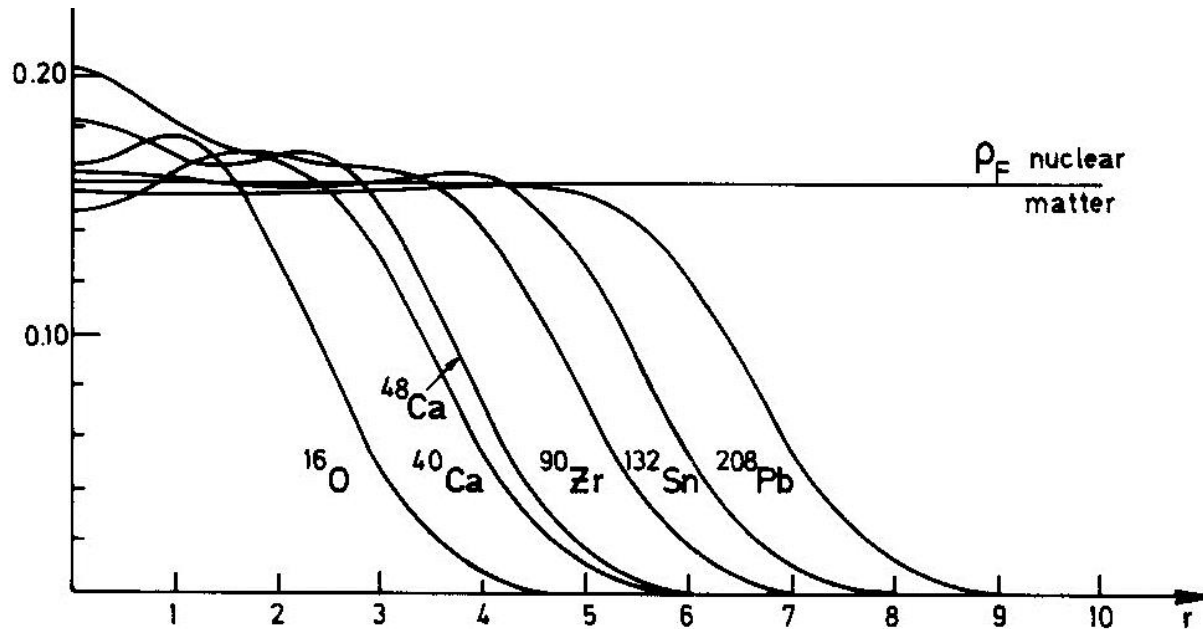
target

if reaction takes place when two nuclei overlap with each other:

$$\sigma_I \sim \pi [R_I(P) + R_I(T)]^2$$

$$\longrightarrow R_I(P)$$

stable nuclei



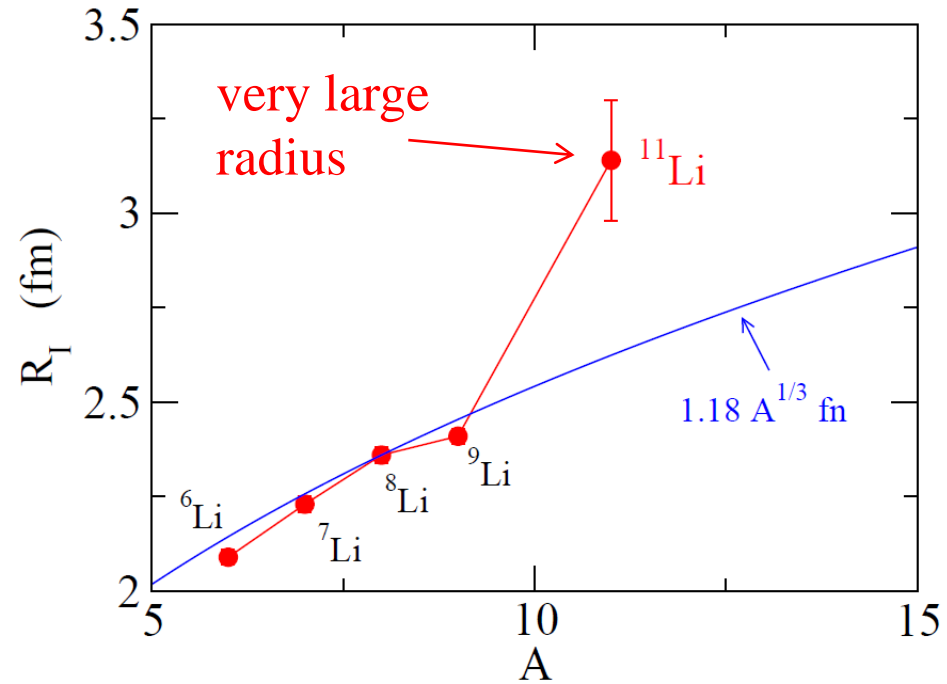
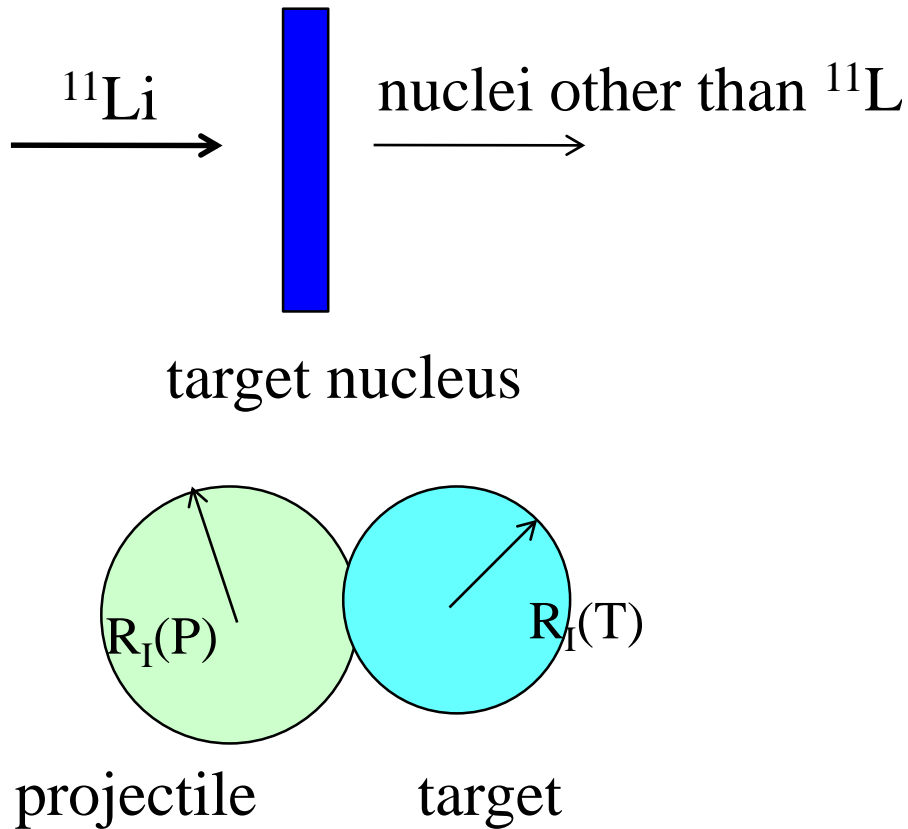
$$\rho(r) = \frac{\rho_0}{1 + \exp((r - R_0)/a)}$$

$$\rho_0 \sim 0.17 \text{ (fm}^{-3}\text{)}$$

$$R_0 \sim 1.1 \times A^{1/3} \text{ (fm)} \quad \leftarrow$$

$$a \sim 0.57 \text{ (fm)}$$

Start of a research on unstable nuclei: interaction cross sections (1985)

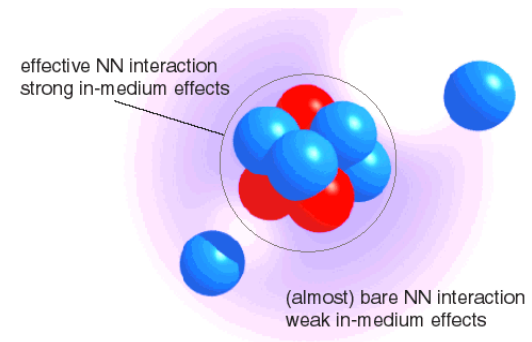


I. Tanihata et al., PRL55('85)2676

if reaction takes place when two nuclei overlap with each other:

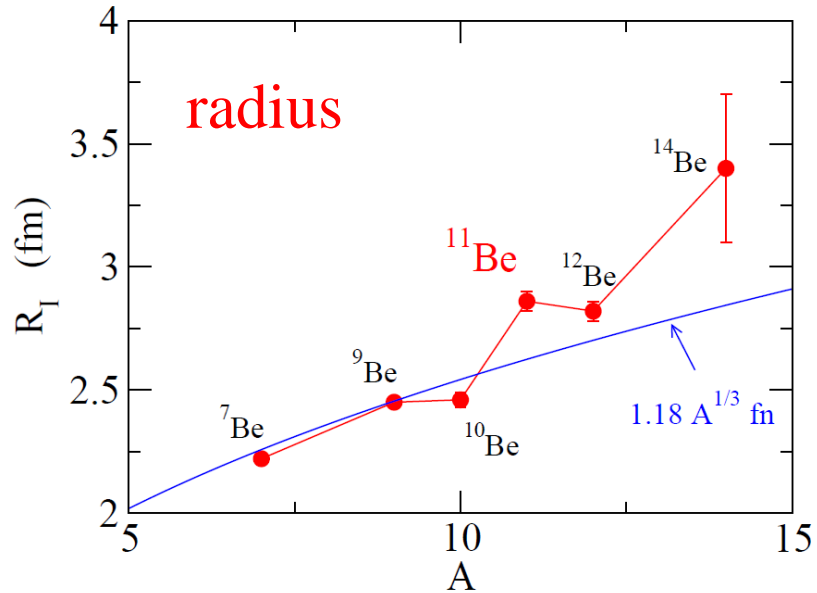
$$\sigma_I \sim \pi [R_I(P) + R_I(T)]^2$$

$$\longrightarrow R_I(P)$$



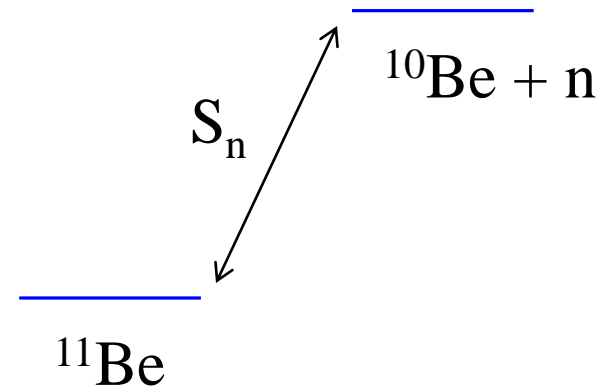
One neutron halo nuclei

A typical example: $^{11}_4\text{Be}_7$



I. Tanihata et al.,
PRL55('85)2676; PLB206('88)592

One neutron separation energy



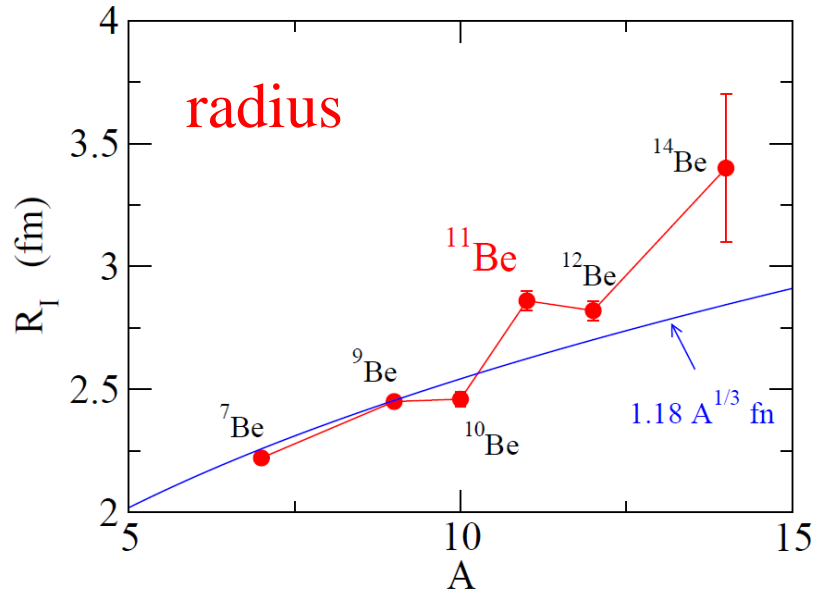
$$S_n = 504 \pm 6 \text{ keV}$$

very small

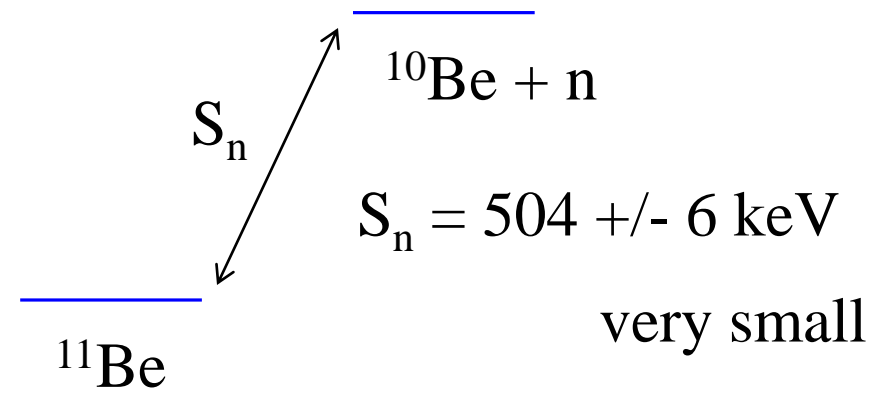
cf. $S_n = 6.81 \text{ MeV}$
for ^{10}Be

One neutron halo nuclei

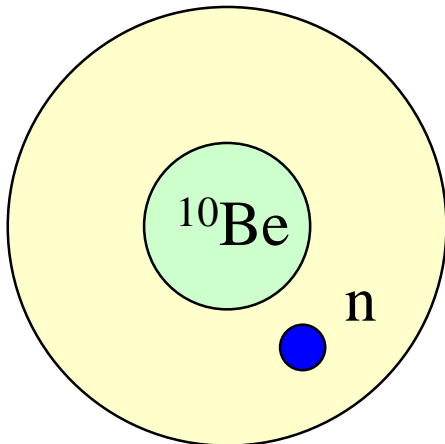
A typical example: $^{11}_4\text{Be}_7$



One neutron separation energy



Interpretation: a weakly bound neutron surrounding ^{10}Be



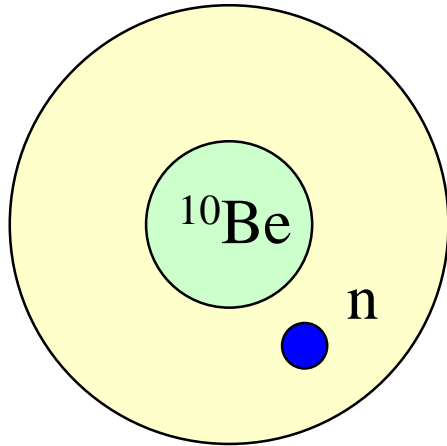
$$\psi(r) \sim \exp(-\kappa r) \quad \kappa = \sqrt{2m|\epsilon|/\hbar^2}$$

weakly bound system



large spatial extension of density (halo structure)

Interpretation: a weakly bound neutron surrounding ^{10}Be



$$\psi(r) \sim \exp(-\kappa r) \quad \kappa = \sqrt{2m|\epsilon|/\hbar^2}$$

weakly bound system

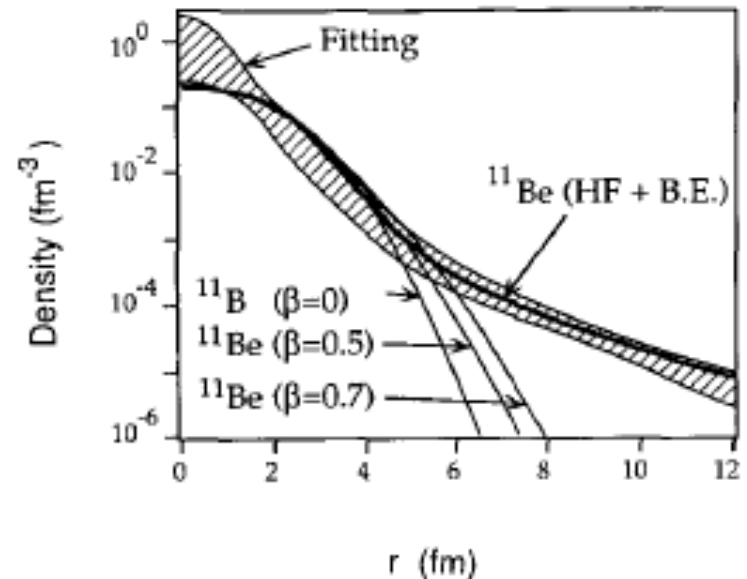


large spatial extension of density (halo structure)

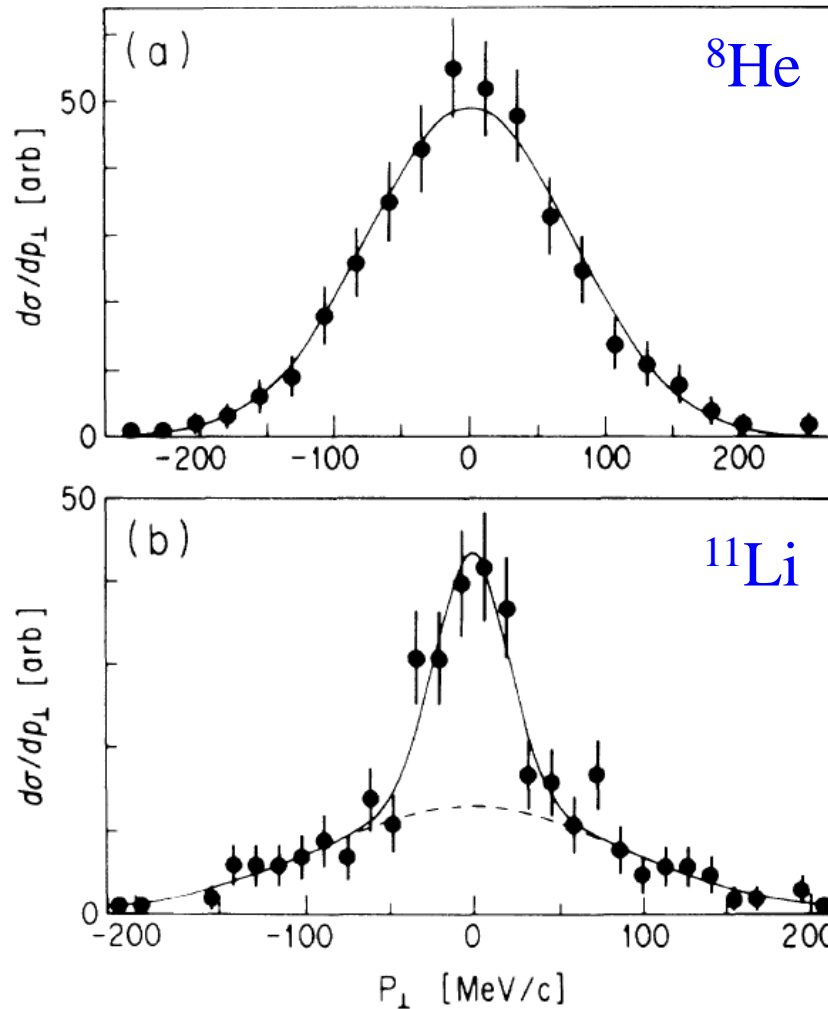
Density distribution which explains the experimental reaction cross section



lunar halo
(a thin ring around moon)



Momentum distribution



$$S_{2n} \sim 2.1 \text{ MeV}$$

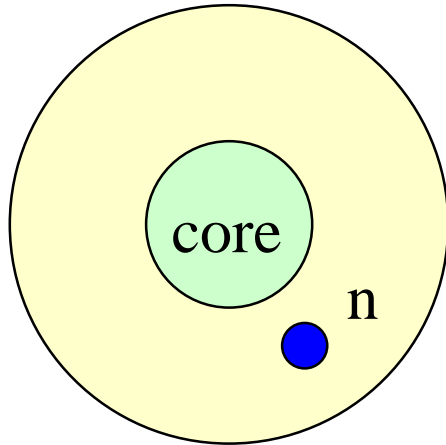
$$S_{2n} \sim 300 \text{ keV}$$

a narrow mom. distribution
when weakly bound and
thus a large spatial extension

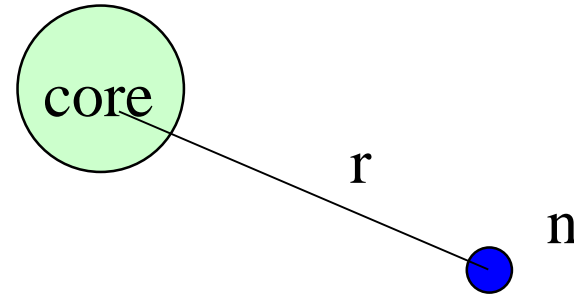
↔ neutron halo

FIG. 1. Transverse-momentum distributions of (a) ^6He fragments from reaction $^8\text{He}+\text{C}$ and (b) ^9Li fragments from reaction $^{11}\text{Li}+\text{C}$. The solid lines are fitted Gaussian distributions. The dotted line is a contribution of the wide component in the ^9Li distribution.

Properties of single-particle motion: bound state



assume a 2body system with a core nucleus and a valence neutron



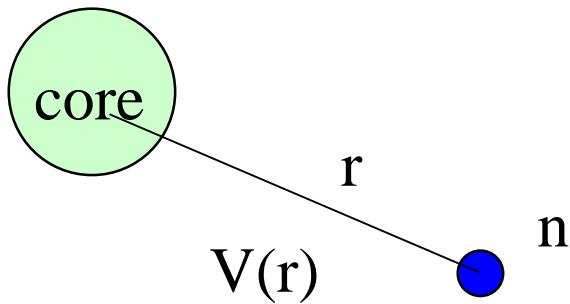
consider a spherical potential $V(r)$ as a function of r

cf. mean-field potential:

$$V(r) \sim \int v(r, r') \rho(r') dr'$$

Hamiltonian for the relative motion

$$H = -\frac{\hbar^2}{2\mu} \nabla^2 + V(r)$$

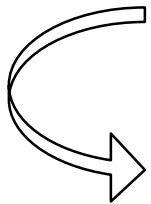


Hamiltonian for the relative motion

$$H = -\frac{\hbar^2}{2\mu}\nabla^2 + V(r)$$

For simplicity, let us ignore the spin-orbit interaction
(the essence remains the same even if no spin-orbit interaction)

$$\Psi_{lm}(r) = \frac{u_l(r)}{r} Y_{lm}(\hat{r})$$



$$\left[-\frac{\hbar^2}{2\mu} \frac{d^2}{dr^2} + \frac{l(l+1)\hbar^2}{2\mu r^2} + V(r) - \epsilon_l \right] u_l(r) = 0$$

Boundary condition for bound states

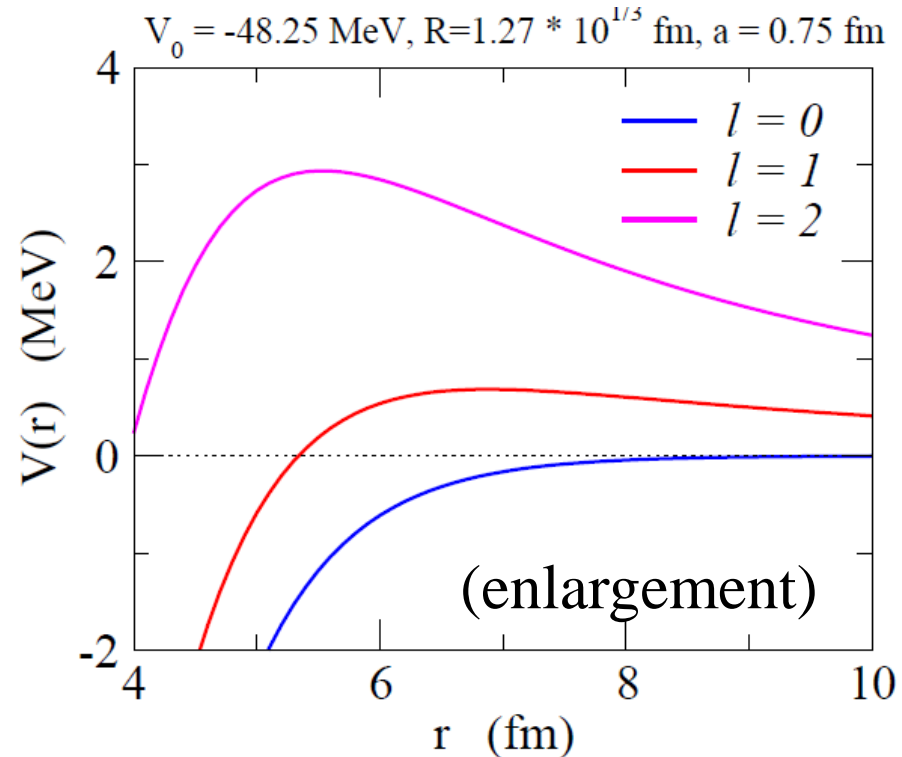
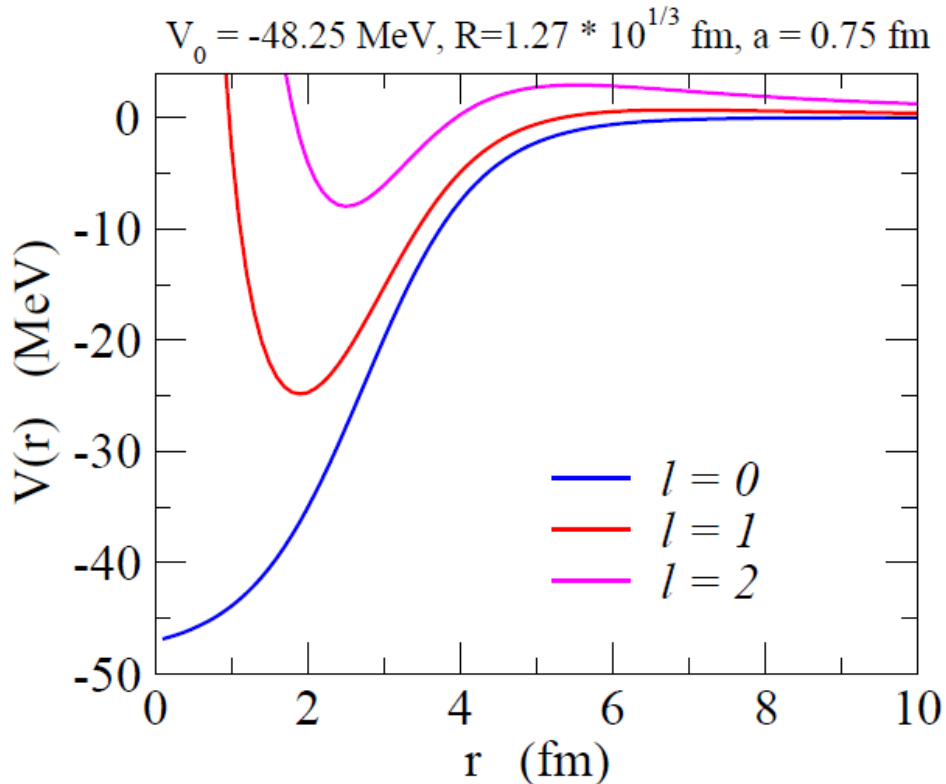
$$\begin{aligned} u_l(r) &\sim r^{l+1} && (r \sim 0) \\ &\rightarrow e^{-\kappa r} && (r \rightarrow \infty) \end{aligned}$$

* For a more consistent treatment, a modified spherical Bessel function has to be used

Angular momentum and halo phenomenon

$$\left[-\frac{\hbar^2}{2\mu} \frac{d^2}{dr^2} + \frac{l(l+1)\hbar^2}{2\mu r^2} + V(r) - \epsilon_l \right] u_l(r) = 0$$

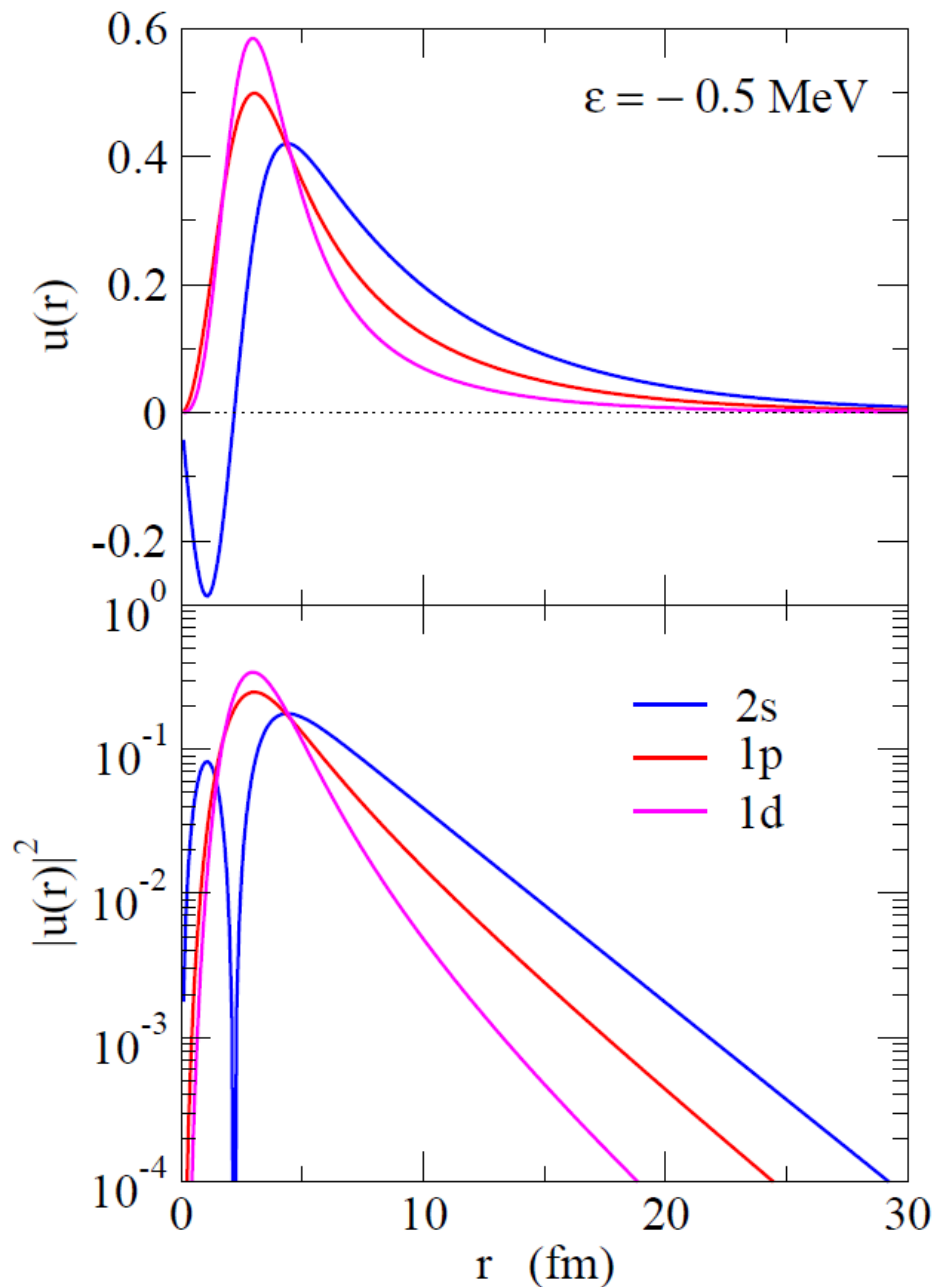
Centrifugal potential



Height of centrifugal barrier: 0 MeV ($l=0$), 0.69 MeV ($l=1$), 2.94 MeV ($l=2$)

Wave function

Change V_0 for each l so that $\varepsilon = -0.5$ MeV



$l = 0$: a long tail

$l = 2$: localization

$l = 1$: intermediate

root-mean-square radius

$$\sqrt{\langle r^2 \rangle} = \sqrt{\int_0^\infty dr r^2 u_l(r)^2}$$

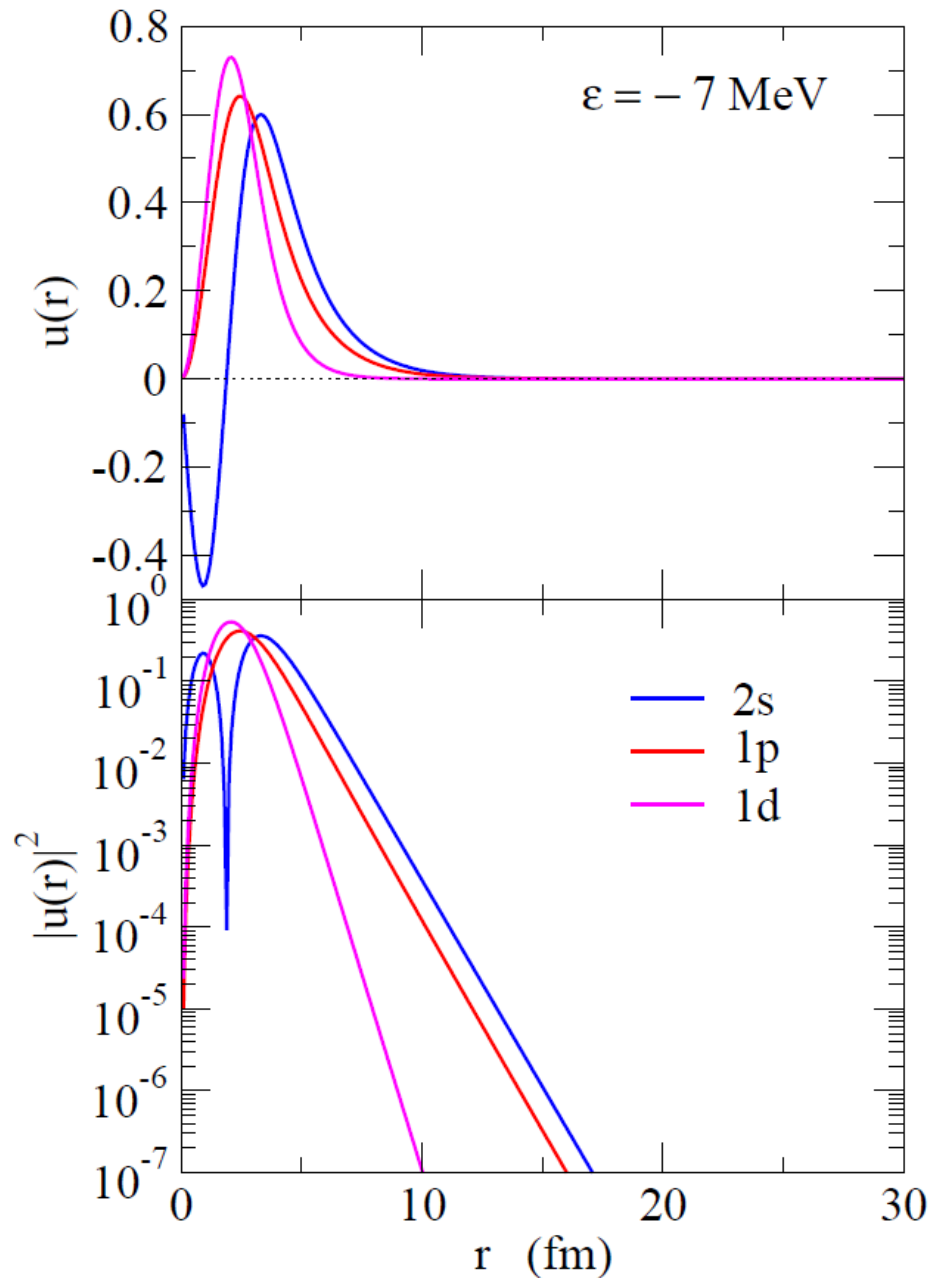
7.17 fm ($l = 0$)

5.17 fm ($l = 1$)

4.15 fm ($l = 2$)

Wave function

For $\varepsilon = -7$ MeV



Wave function: localized for
all l

root-mean-square radius:

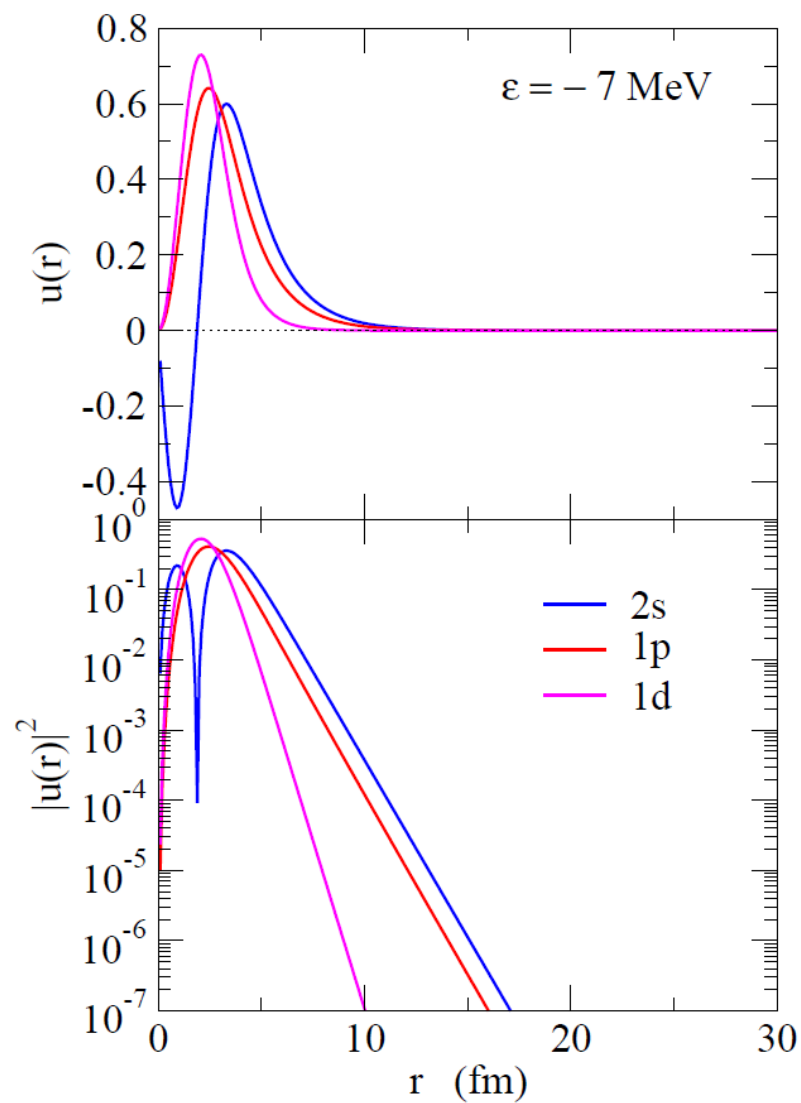
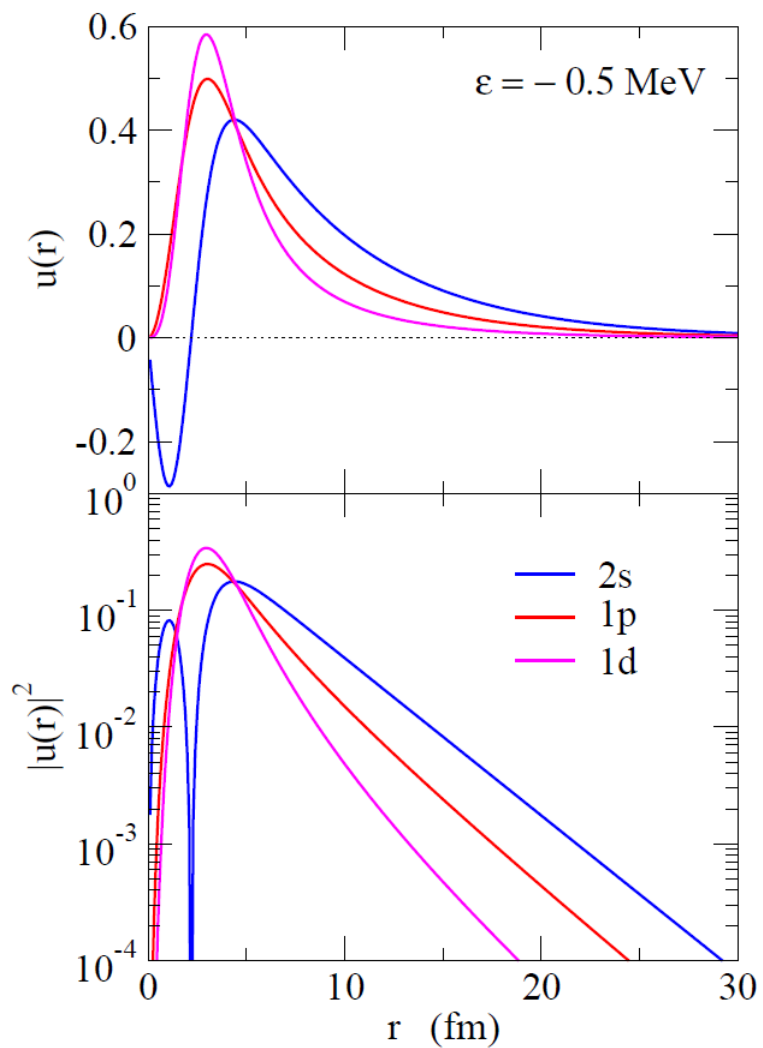
$$\sqrt{\langle r^2 \rangle} = \sqrt{\int_0^\infty dr r^2 u_l(r)^2}$$

3.58 fm ($l = 0$)

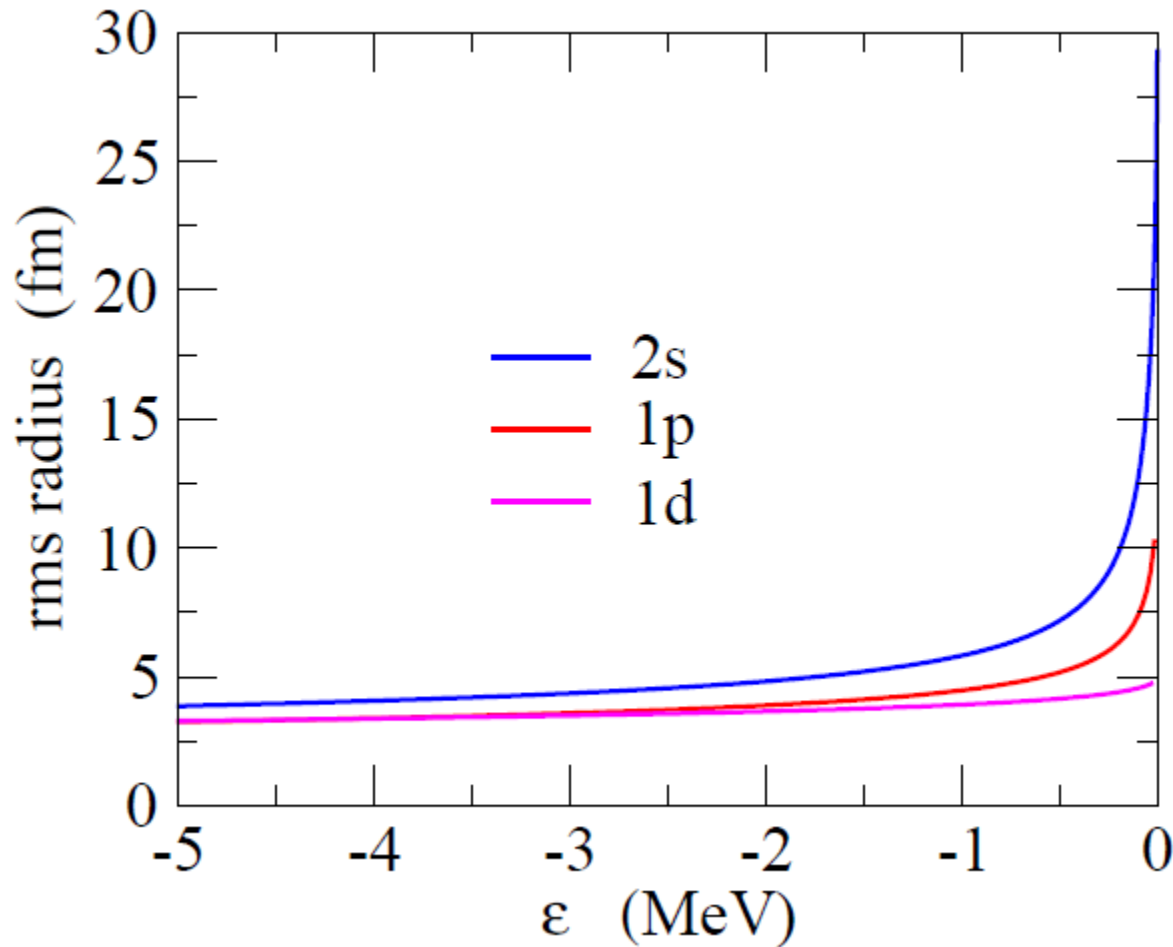
3.05 fm ($l = 1$)

3.14 fm ($l = 2$)

Wave functions



$$\langle r^2 \rangle \propto \begin{cases} 1/|\epsilon_0| & (l=0) \\ 1/\sqrt{|\epsilon_1|} & (l=1) \\ \text{const.} & (l=2) \end{cases}$$

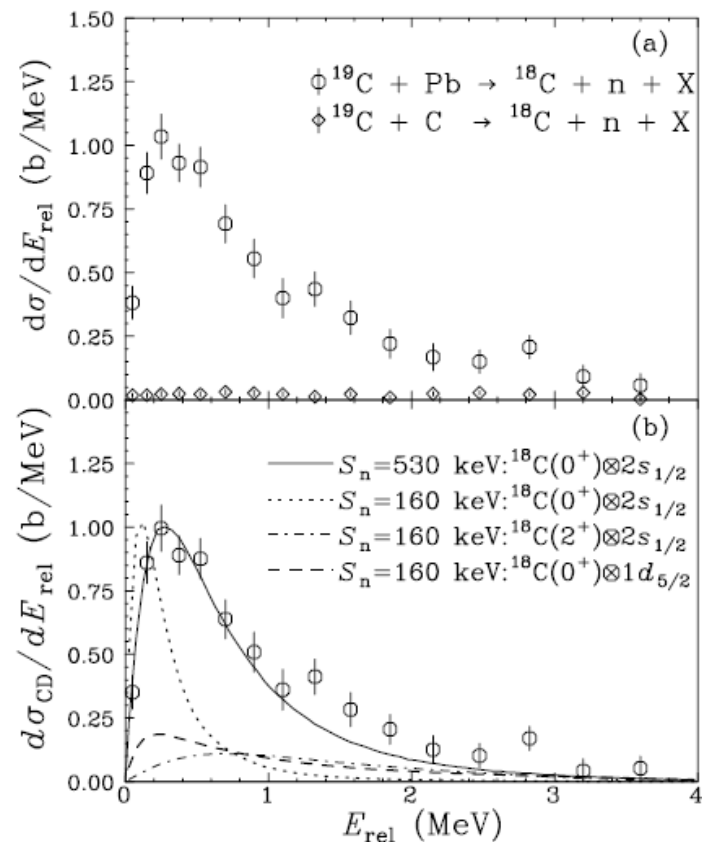


Radius: diverges for $l=0$ and 1 in the zero energy limit

Halo (a very large radius) happens only for $l=0$ or 1

Other candidates for 1n halo nuclei

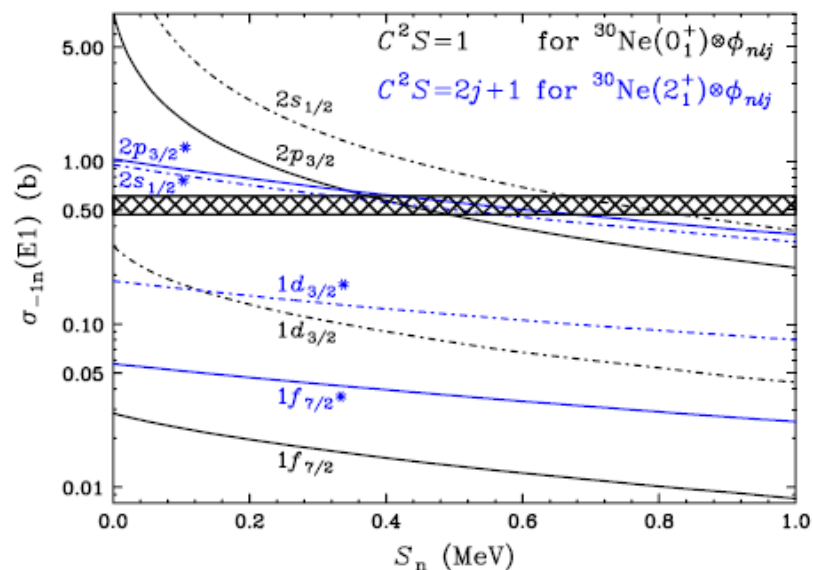
^{19}C : $S_n = 0.58(9)$ MeV



Coulomb breakup of ^{19}C

T. Nakamura et al., PRL83('99)1112

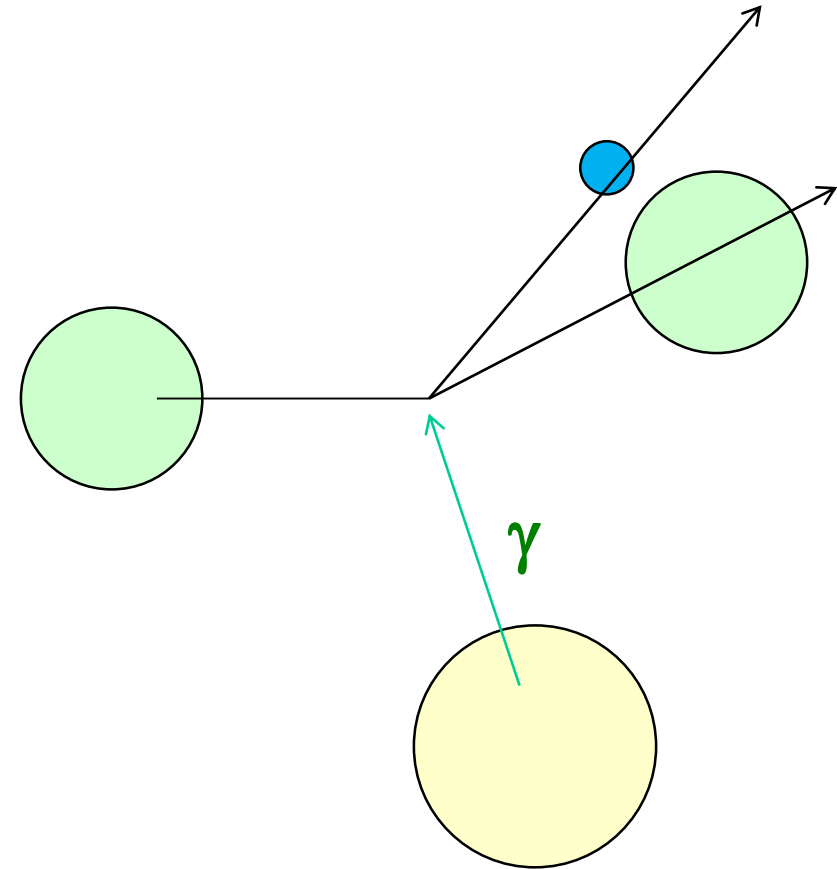
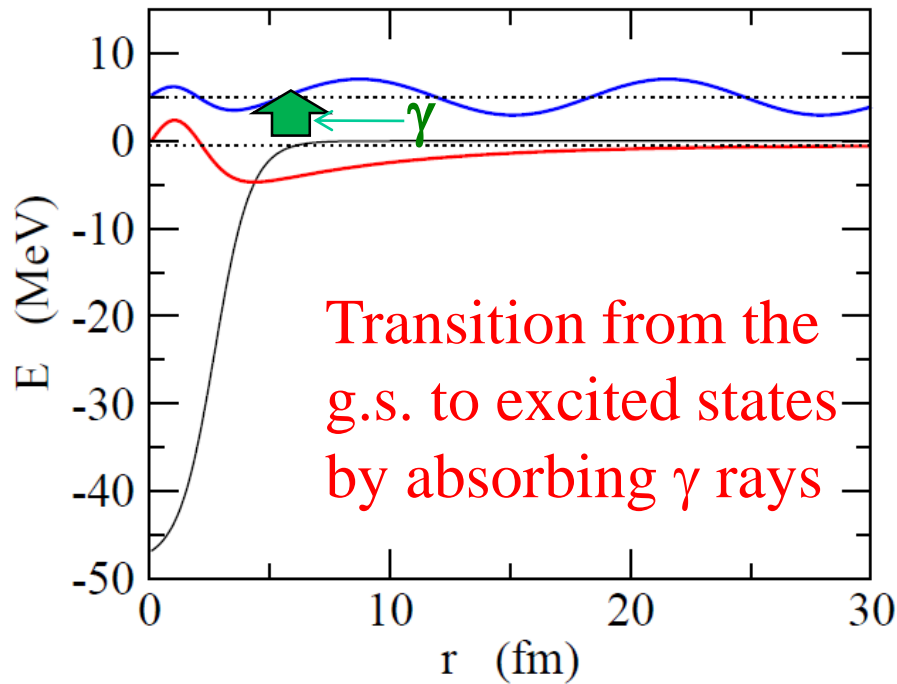
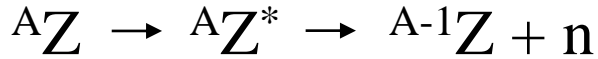
^{31}Ne : $S_n = 0.29 \pm 1.64$ MeV



Large Coulomb breakup
cross sections

T. Nakamura et al.,
PRL103('09)262501

Coulomb breakup of 1n halo nuclei

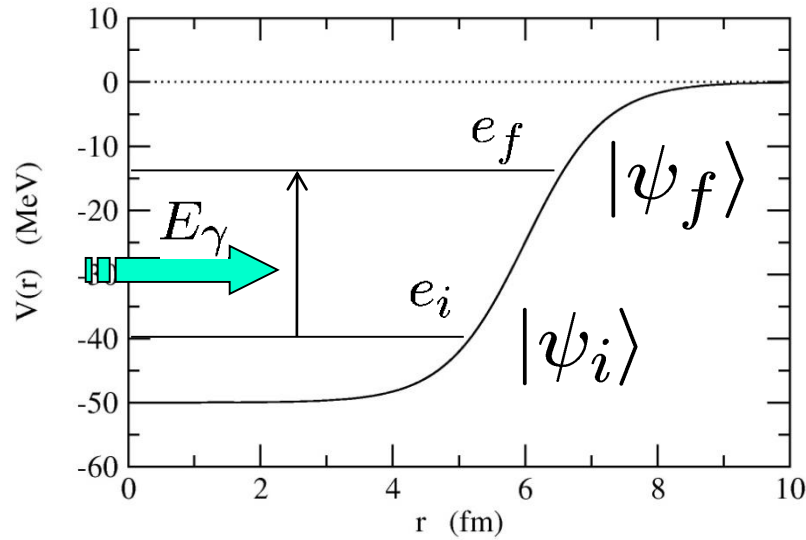


breakup if excited to
continuum states

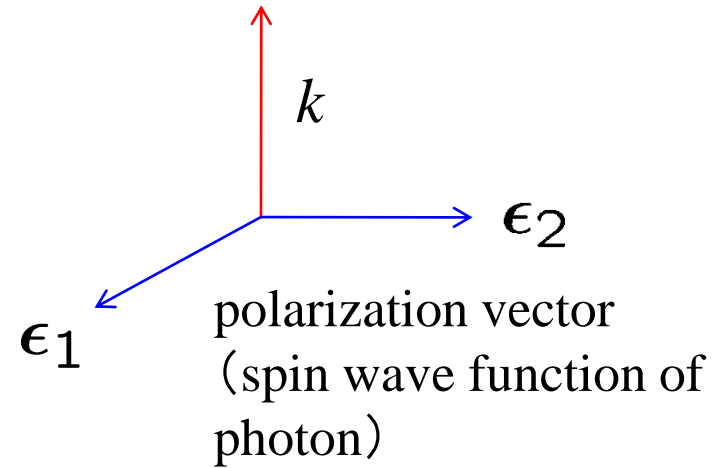


excitations due to the Coulomb
field from the target nucleus

Electromagnetic transitions



photon



initial state: $|\psi_i\rangle |n_{k\alpha} = 1\rangle$



State of nucleus: Ψ_i ,
+ one photon with
momentum k , and
polarization α
($\alpha = 1$ or 2)

transition



H_{int}
(interaction between
a nucleus and EM field)

final state: $|\psi_f\rangle |n_{k\alpha} = 0\rangle$

(note) time-dependent perturbation theory

$$H_{\text{int}} = \frac{1}{Am} \cdot \frac{Ze}{c} \mathbf{A} \cdot \mathbf{p}$$

$$\mathbf{A}(\mathbf{r}, t) = \sum_{\alpha} \int \frac{d\mathbf{k}}{2\pi} \frac{\hbar c}{\sqrt{\hbar\omega}} \left[a_{\mathbf{k}\alpha} \boldsymbol{\epsilon}_{\alpha} e^{-i\omega t} + a_{\mathbf{k}\alpha}^{\dagger} \boldsymbol{\epsilon}_{\alpha} e^{i\omega t} \right] = \mathbf{A}(t) \quad (\text{dipole approximation})$$

transition probability per unit time due to: $V(\mathbf{r}, t) = F(\mathbf{r}) e^{\pm i\omega t}$
(for a transition to a single state)

$$\Gamma_{i \rightarrow f} = \frac{2\pi}{\hbar} |\langle f | F | i \rangle|^2 \delta(e_f - e_i \pm \hbar\omega) \quad \text{Fermi's Golden Rule}$$

application to the present problem:

$$\Gamma_{i \rightarrow f} = \frac{1}{2\pi\hbar} \left(\frac{Ze}{A+1} \right)^2 (e_f - e_i) \left| \langle \psi_f | z | \psi_i \rangle \right|^2 \delta(e_f - e_i - \hbar\omega)$$

(note) photo-absorption cross section if Γ is divided by the photon flux $c/(2\pi)^3$:

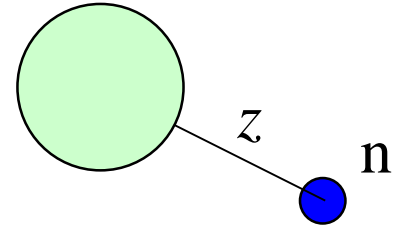
$$\sigma_{\gamma} = \frac{4\pi^2}{\hbar c} \left(\frac{Ze}{A+1} \right)^2 (e_f - e_i) \left| \langle \psi_f | z | \psi_i \rangle \right|^2 \delta(e_f - e_i - \hbar\omega)$$

Application to the present problem:

$$\Gamma_{i \rightarrow f} = \frac{1}{2\pi\hbar} \left(\frac{Ze}{A+1} \right)^2 (e_f - e_i) \left| \langle \psi_f | z | \psi_i \rangle \right|^2 \delta(e_f - e_i - \hbar\omega)$$



$$P_{i \rightarrow f} \sim \left| \langle \psi_f | z | \psi_i \rangle \right|^2$$



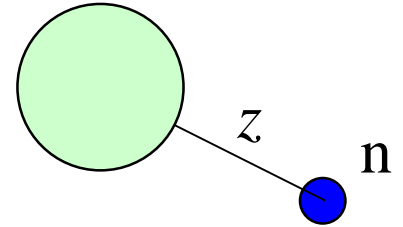
$$\sum_f P_{i \rightarrow f} =$$

Application to the present problem:

$$\Gamma_{i \rightarrow f} = \frac{1}{2\pi\hbar} \left(\frac{Ze}{A+1} \right)^2 (e_f - e_i) \left| \langle \psi_f | z | \psi_i \rangle \right|^2 \delta(e_f - e_i - \hbar\omega)$$



$$P_{i \rightarrow f} \sim \left| \langle \psi_f | z | \psi_i \rangle \right|^2$$



$$\begin{aligned} \sum_f P_{i \rightarrow f} &= \sum_f \langle \psi_i | z | \psi_f \rangle \langle \psi_f | z | \psi_i \rangle \\ &= \langle \psi_i | z^2 | \psi_i \rangle \end{aligned}$$



large transition probability if the spatial extension in z is large

Wigner-Eckart theorem and reduced transition probability

$$\sigma_\gamma = \frac{16\pi^3}{3\hbar c} \left(\frac{Ze}{A+1} \right)^2 E_\gamma |\langle \psi_f | r Y_{10} | \psi_i \rangle|^2 \delta(e_f - e_i - E_\gamma)$$

$$E_\gamma = e_f - e_i = \hbar\omega$$

$$\begin{aligned} |\langle \psi_f | r Y_{10} | \psi_i \rangle|^2 &\rightarrow \frac{1}{2l+1} \sum_{m,m'} |\langle \psi_{l'm'} | r Y_{10} | \psi_{lm} \rangle|^2 \\ &= \frac{1}{3} \cdot \frac{1}{2l+1} |\langle \psi_{l'} || r Y_1 || \psi_l \rangle|^2 \end{aligned}$$



$$\begin{aligned} \sigma_\gamma &= \frac{16\pi^3}{9\hbar c} E_\gamma \cdot \frac{1}{2l+1} |\langle \psi_f || e_{E1} r Y_1 || \psi_i \rangle|^2 \delta(e_f - e_i - E_\gamma) \\ &= \frac{16\pi^3}{9\hbar c} E_\gamma \cdot \frac{dB(E1)}{dE_\gamma} \end{aligned}$$

Reduced transition probability

$$\frac{dB(E1)}{dE_\gamma} = \frac{1}{2l+1} |\langle \psi_f || e_{E1} r Y_1 || \psi_i \rangle|^2 \delta(e_f - e_i - E_\gamma)$$

E1 effective charge

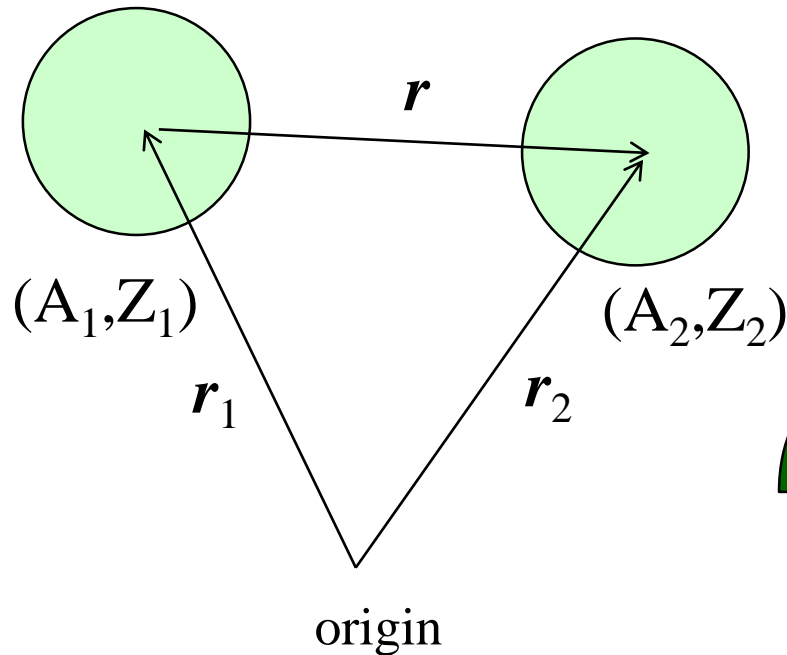
$$\sigma_\gamma = \frac{16\pi^3}{3\hbar c} \left(\frac{Ze}{A+1} \right)^2 (e_f - e_i) \left| \langle \psi_f | r Y_{10} | \psi_i \rangle \right|^2 \delta(e_f - e_i - \hbar\omega)$$

dipole operator:

$$\hat{D}_\mu = e_{E1} \cdot r Y_{1\mu}(\theta, \phi)$$

$$e_{E1} = \frac{Z}{A+1} e$$

Distribution of charges
measured from the center of mass



$$Z_1(\mathbf{r}_1 - \mathbf{R}) + Z_2(\mathbf{r}_2 - \mathbf{R})$$

$$\mathbf{R} = \frac{A_1 \mathbf{r}_1 + A_2 \mathbf{r}_2}{A_1 + A_2}$$

$$\begin{aligned} &= \dots \\ &= \frac{Z_1 A_2 - Z_2 A_1}{A_1 + A_2} (\mathbf{r}_1 - \mathbf{r}_2) \\ &= \frac{Z_1 A_2 - Z_2 A_1}{A_1 + A_2} \mathbf{r} \end{aligned}$$

$$e_{E1} = \frac{Z_1 A_2 - Z_2 A_1}{A_1 + A_2} e$$

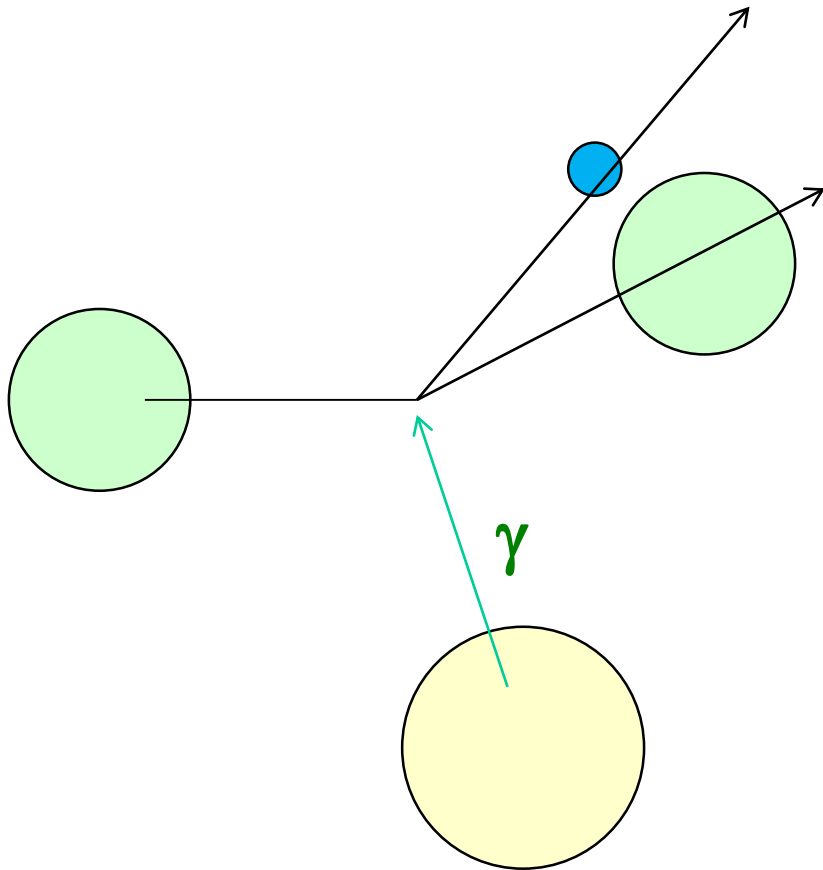
(a general formula for 2-body)

Coulomb breakup cross sections

$$\sigma_{\gamma} = \frac{16\pi^3}{9\hbar c} E_{\gamma} \cdot \frac{dB(E1)}{dE_{\gamma}}$$



$$\frac{d\sigma_{\gamma}}{dE_{\gamma}} \sim \frac{16\pi^3}{9\hbar c} \cdot \frac{dB(E1)}{dE_{\gamma}}$$



In actual **nuclear reactions**,
absorption of virtual photons
rather than real photons

$$\frac{d\sigma}{dE_{\text{ex}}} \sim \frac{16\pi^3}{9\hbar c} \cdot N_{E1}(E_{\text{ex}}) \cdot \frac{dB(E1)}{dE_{\text{ex}}}$$

of virtual photon

See: C.A. Bertulani and P. Danielwicz,
“Introduction to Nuclear Reactions”
for more details


Simple estimate of E1 strength distribution (analytic model)

Transition from an $l = 0$ to an $l = 1$ states:


WF for the initial state: $\Psi_i(\mathbf{r}) = \sqrt{2\kappa} \frac{e^{-\kappa r}}{r} Y_{00}(\hat{\mathbf{r}})$ $\kappa = \sqrt{\frac{2\mu|E_b|}{\hbar^2}}$

WF for the final state: $\Psi_f(\mathbf{r}) = \sqrt{\frac{2\mu k}{\pi\hbar^2}} j_1(kr) Y_{1m}(\hat{\mathbf{r}})$ $j_1(kr)$: spherical Bessel function

$$k = \sqrt{\frac{2\mu E_c}{\hbar^2}}$$


$$\frac{dB(E1)}{dE} = \frac{3}{4\pi} e_{E1}^2 \left| \int_0^\infty r^2 dr r \cdot \frac{\sqrt{2\kappa} e^{-\kappa r}}{r} \cdot \sqrt{\frac{2\mu k}{\pi\hbar^2}} j_1(kr) \right|^2$$

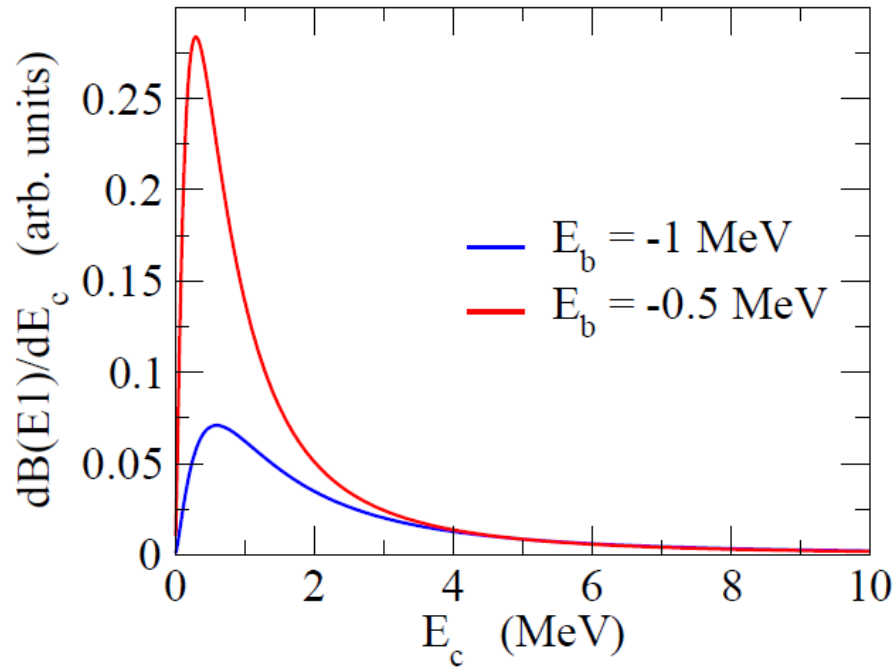
The integral can be performed analytically


$$\frac{dB(E1)}{dE} = \frac{3\hbar^2}{\pi^2\mu} e_{E1}^2 \frac{\sqrt{|E_b|} E_c^{3/2}}{(|E_b| + E_c)^4}$$

Refs. (for more general l_i and l_f)

- M.A. Nagarajan, S.M. Lenzi, A. Vitturi, Eur. Phys. J. A24('05)63
- S. Typel and G. Baur, NPA759('05)247

$$\frac{dB(E1)}{dE} = \frac{3\hbar^2}{\pi^2\mu} e_{E1}^2 \frac{\sqrt{|E_b|} E_c^{3/2}}{(|E_b| + E_c)^4}$$



peak position: $E_c = \frac{3}{5} |E_b|$
 $(E_x = E_c - E_b = \frac{8}{5} |E_b|)$

peak height: $\propto 1/|E_b|^2$

Total transition probability:

$$B(E1) = S_0 = \frac{3\hbar^2 e_{E1}^2}{16\pi^2\mu |E_b|}$$



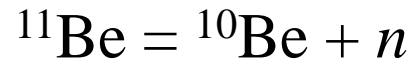
➤ a high and sharp peak as the bound state energy, $|E_b|$, becomes small

➤ As the bound state energy, $|E_b|$, gets small, the peak appears at a low energy

$$E_{\text{peak}} = 0.28 \text{ MeV } (E_b = -0.5 \text{ MeV})$$

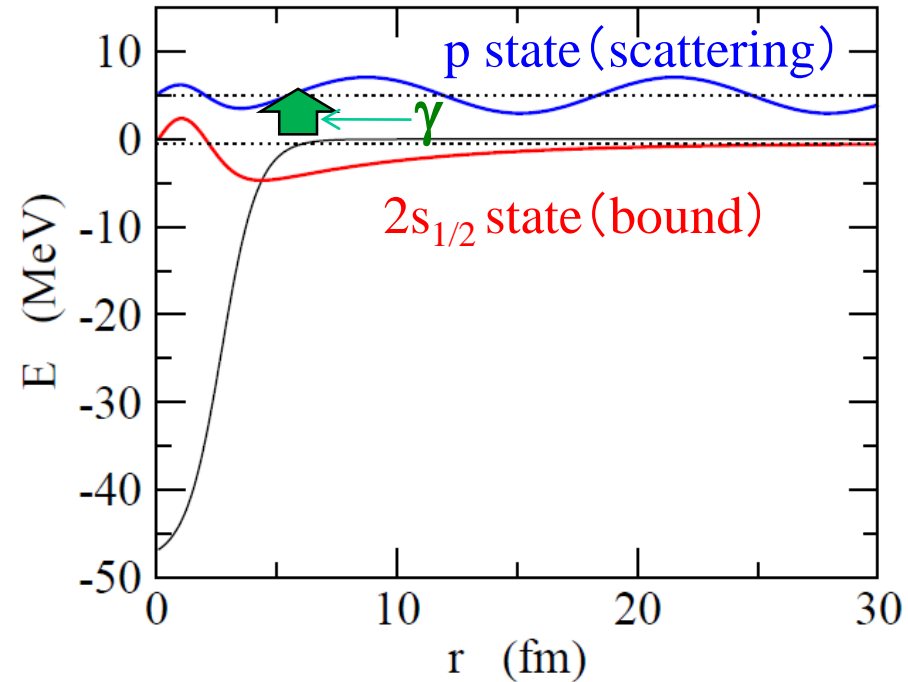
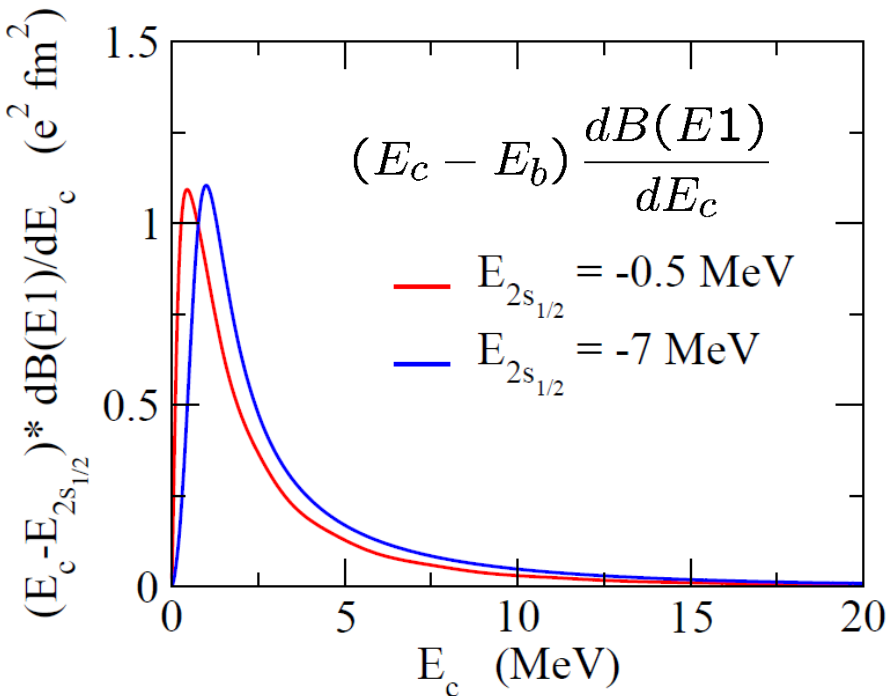
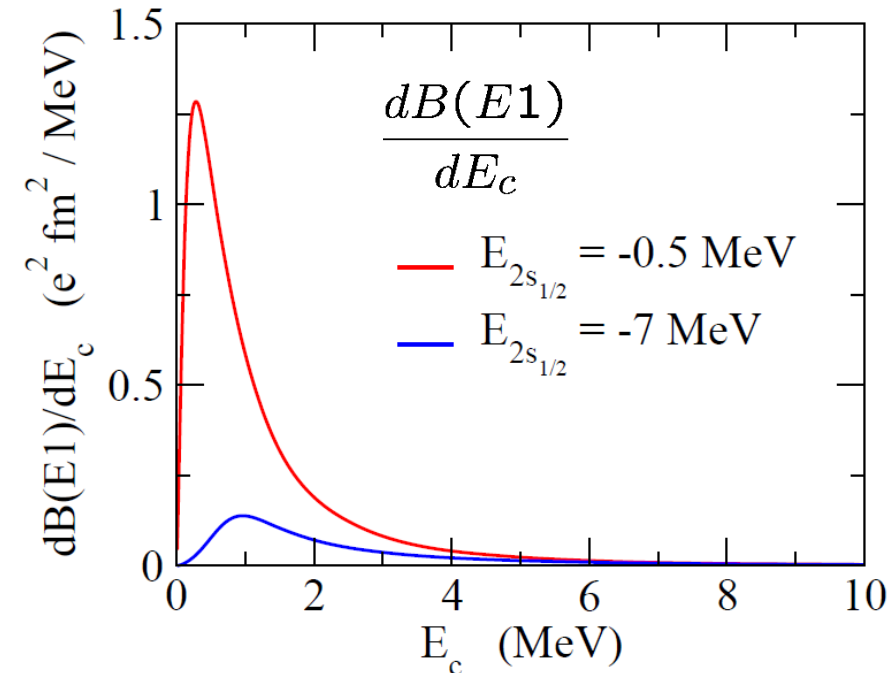
$$\text{cf. } \frac{3}{5} |E_b| = 0.3 \text{ MeV}$$

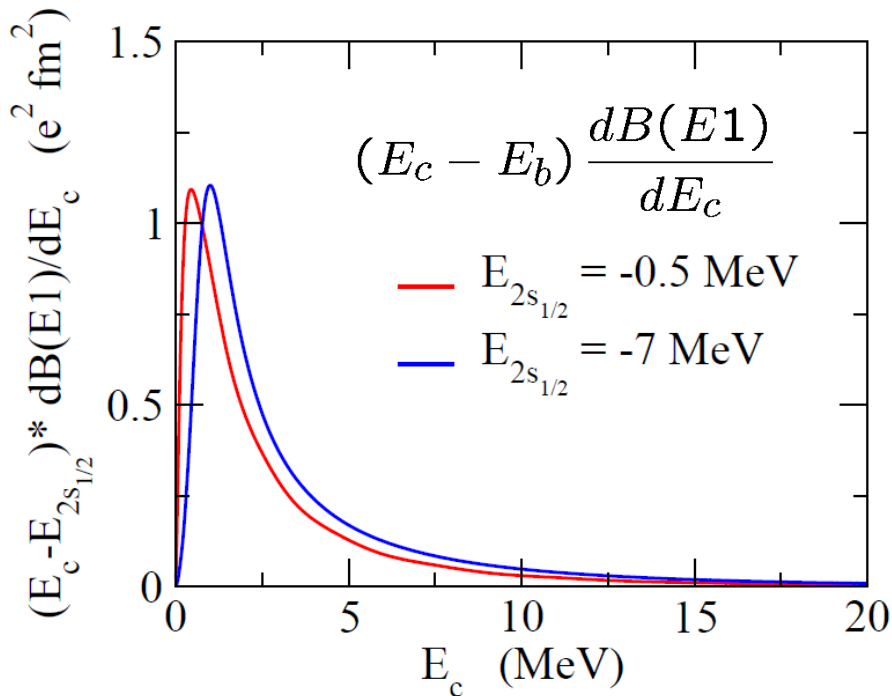
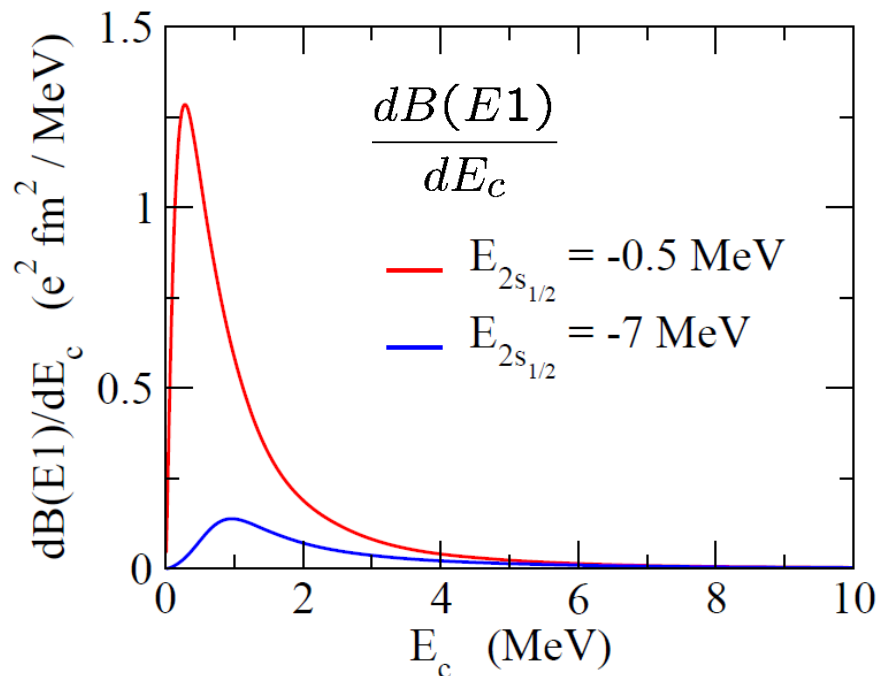
Actual numerical calculations with a Woods-Saxon potential



transition from the $2s_{1/2}$ state (bound) to the p-wave ($l = 1$) state

Comparison between a weakly-bound case and a strongly-bound case





➤ a high and sharp peak as the bound state energy, $|E_b|$, becomes small

$$S_0 = \int_0^\infty dE_c \frac{dB(E1)}{dE_c}$$

$$= 1.53 \text{ e}^2\text{fm}^2 \quad (E_b = -0.5 \text{ MeV})$$

$$0.32 \text{ e}^2\text{fm}^2 \quad (E_b = -7 \text{ MeV})$$

➤ As the bound state energy, $|E_b|$, gets small, the peak appears at a low energy

$$E_{\text{peak}} = 0.28 \text{ MeV} \quad (E_b = -0.5 \text{ MeV})$$

$$0.96 \text{ MeV} \quad (E_b = -7 \text{ MeV})$$

➤ Weak E_b dependence when the transition strength is multiplied by $(E_c - E_b)$

$$S_1 = \int_0^\infty dE_c (E_c - E_b) \frac{dB(E1)}{dE_c}$$

$$= 2.79 \text{ e}^2\text{fm}^2 \text{ MeV} \quad (E_b = -0.5 \text{ MeV})$$

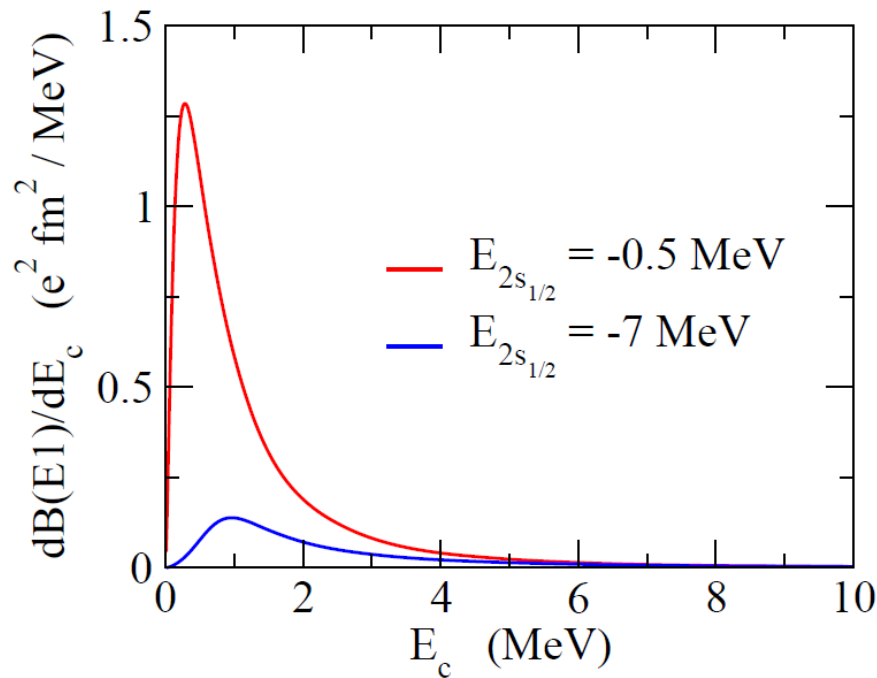
$$3.18 \text{ e}^2\text{fm}^2 \text{ MeV} \quad (E_b = -7 \text{ MeV})$$

Sum Rule

$$S_0 = \int_0^\infty dE_c \frac{dB(E1)}{dE_c} = \frac{3}{4\pi} e_{E1}^2 \langle r^2 \rangle_i$$



Total E1 transition probability: proportional to the g.s. expectation value of r^2



$$S_0 = \int_0^\infty dE_c \frac{dB(E1)}{dE_c} = 1.53 \text{ e}^2 \text{fm}^2 \quad (E_b = -0.5 \text{ MeV})$$
$$0.32 \text{ e}^2 \text{fm}^2 \quad (E_b = -7 \text{ MeV})$$

$$\frac{3}{4\pi} e_{E1}^2 \langle r^2 \rangle_i = 1.62 \text{ e}^2 \text{fm}^2 \quad (E_b = -0.5 \text{ MeV})$$
$$0.41 \text{ e}^2 \text{fm}^2 \quad (E_b = -7 \text{ MeV})$$

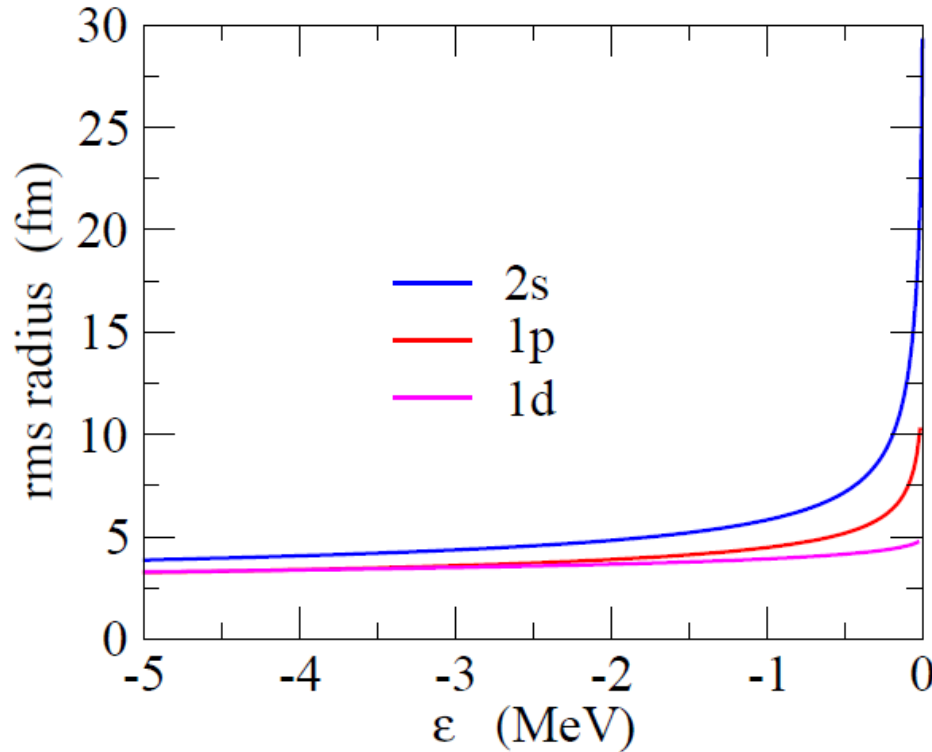
* almost coincide with each other. Small difference due to Pauli forbidden transitions (the transition from 2s to 1p)

Sum Rule

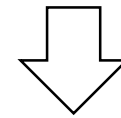
$$S_0 = \int_0^\infty dE_c \frac{dB(E1)}{dE_c} = \frac{3}{4\pi} e_{E1}^2 \langle r^2 \rangle_i$$



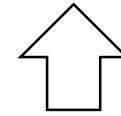
Total E1 transition probability: proportional to the g.s. expectation value of r^2



If the initial state is $l=0$ or $l=1$, the radius increases for weakly bound



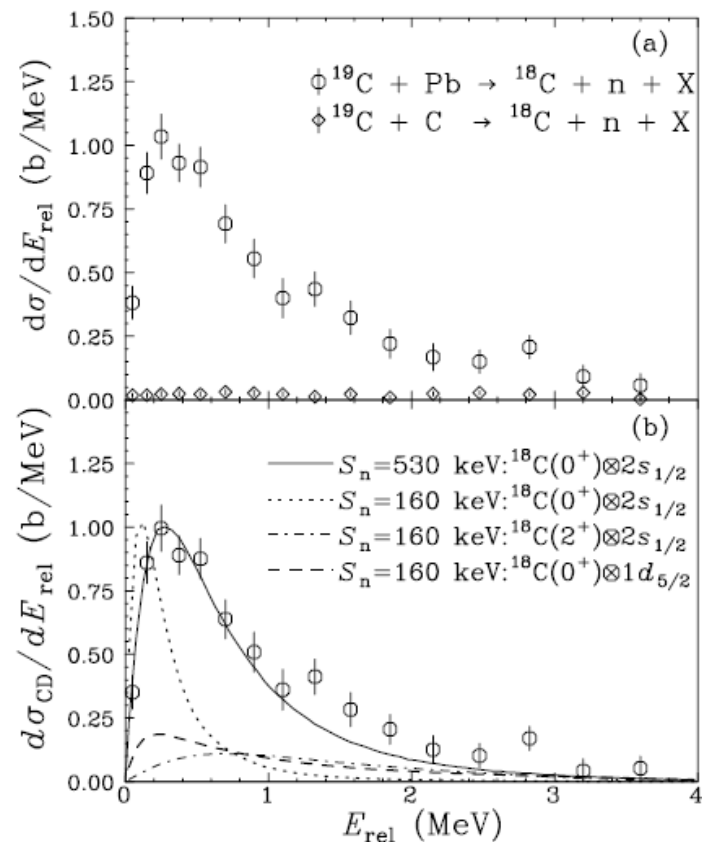
Enhancement of total E1 prob.



Inversely, if a large E1 prob. (or a large Coul. b.u. cross sections) are observed, this indicates $l=0$ or $l=1$ \longrightarrow halo structure

Other candidates for 1n halo nuclei

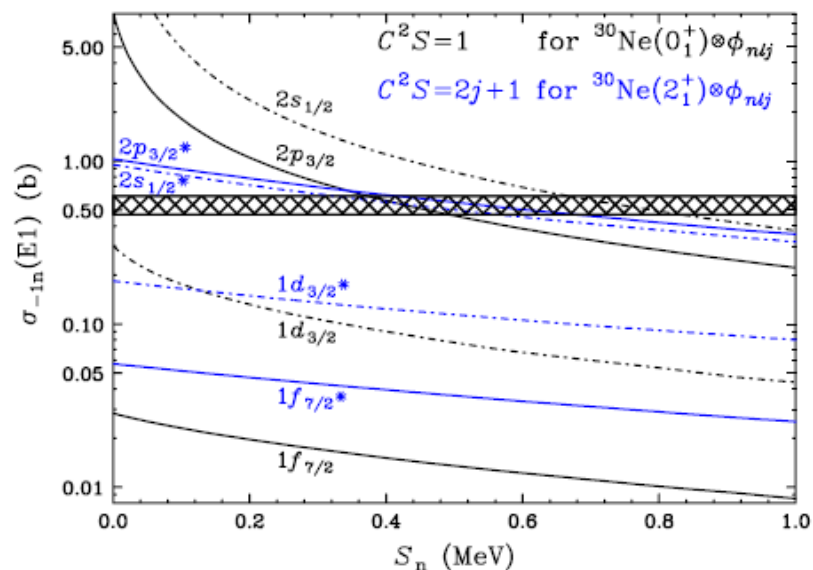
^{19}C : $S_n = 0.58(9)$ MeV



Coulomb breakup of ^{19}C

T. Nakamura et al., PRL83('99)1112

^{31}Ne : $S_n = 0.29 \pm 1.64$ MeV

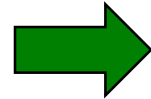
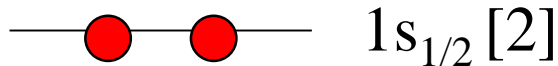
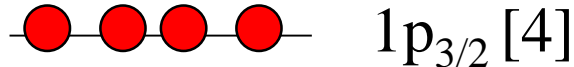
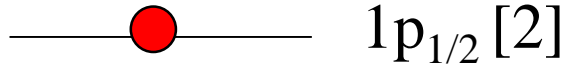


Large Coulomb breakup
cross sections

T. Nakamura et al.,
PRL103('09)262501

Nuclear deformation

With a spherical potential:



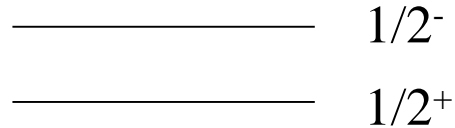
The g.s. of ^{11}Be : $I^\pi = 1/2^-$

very artificial

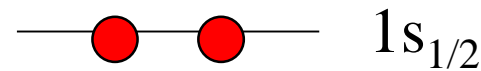
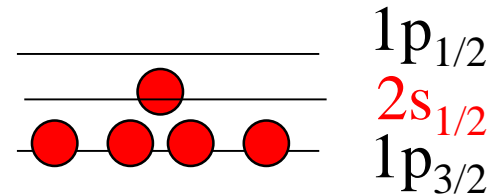
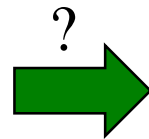


In reality.....

0.32 MeV



^{11}Be



“parity inversion”

What happens if ^{11}Be is deformed?

s.p. motion in a deformed potential

halo : only for $l = 0$ or 1

⇒ however, a possibility is enlarged for a deformed nucleus

deformed potential $V(r, \theta)$ → mixture of angular momenta

e.g.,

$$|d_{5/2}\rangle \rightarrow |d_{5/2}\rangle + |s_{1/2}\rangle + |g_{7/2}\rangle + \dots$$

$$|f_{7/2}\rangle \rightarrow |f_{7/2}\rangle + |p_{3/2}\rangle + |p_{1/2}\rangle + \dots$$

(note) $s_{1/2} : \Omega^\pi = 1/2^+$ only

$p_{1/2} : \Omega^\pi = 1/2^-$ only

$p_{3/2} : \Omega^\pi = 3/2^-$ and $1/2^-$ only

} → possibility of halo
only for s.p. states
with
 $\Omega^\pi = 1/2^+, 1/2^-, 3/2^-$

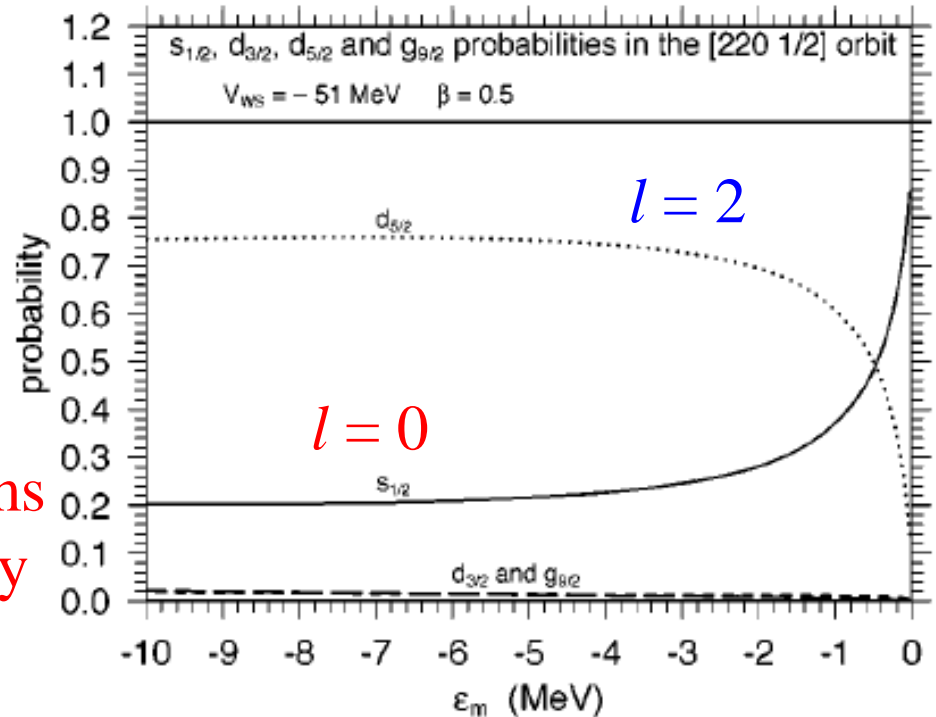
s.p. motion in a deformed potential

$$\begin{aligned} |d_{5/2}\rangle &\rightarrow |d_{5/2}\rangle + |s_{1/2}\rangle + |g_{7/2}\rangle + \dots \\ &\rightarrow |s_{1/2}\rangle \quad (|\epsilon| \rightarrow 0) \end{aligned}$$

T. Misu, W. Nazarewicz,
and S. Aberg, NPA614('97)44
(deformed square well)

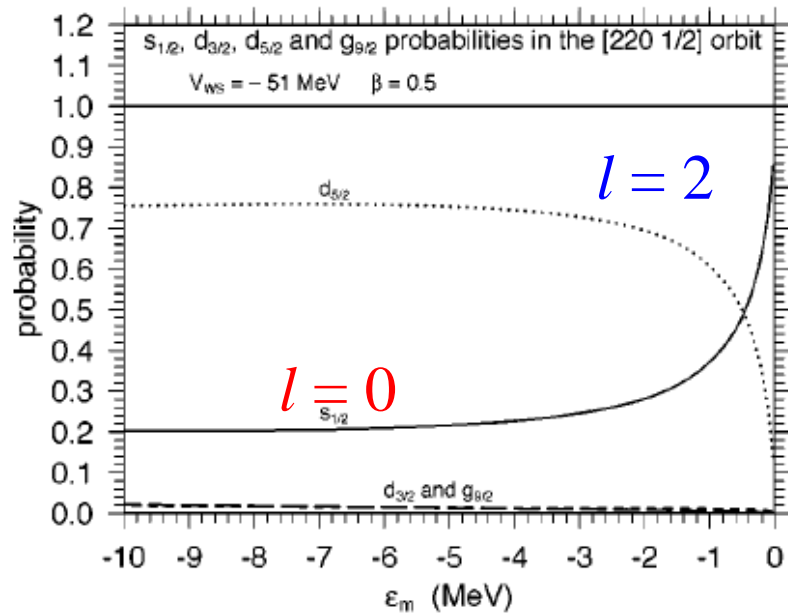
When weakly bound, the $l=0$ terms
becomes dominant even for a very
small deformation

(in the zero binding limit,
100% of $l=0$ component)

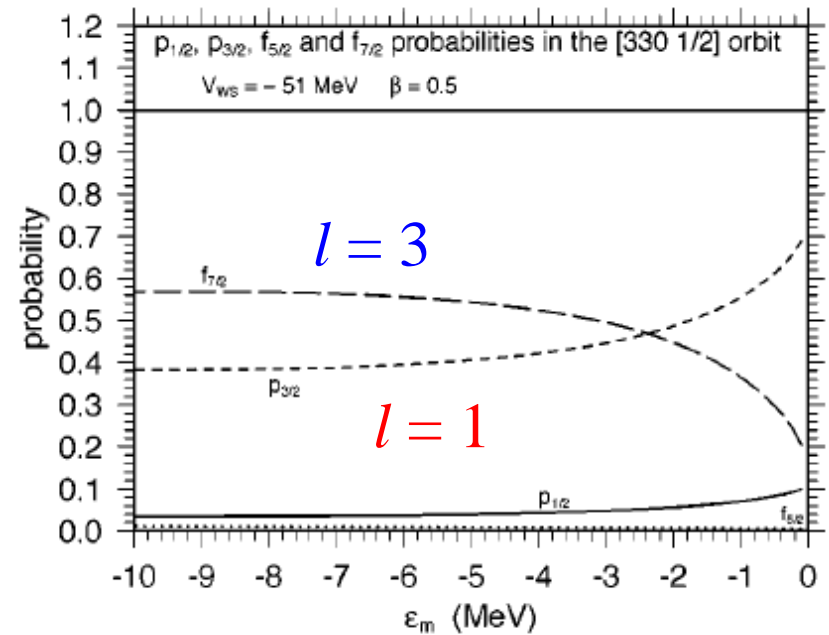


I. Hamamoto, PRC69('04)041306(R)
(deformed Woods-Saxon)

s-wave dominance phenomenon



I. Hamamoto, PRC69('04)041306(R)

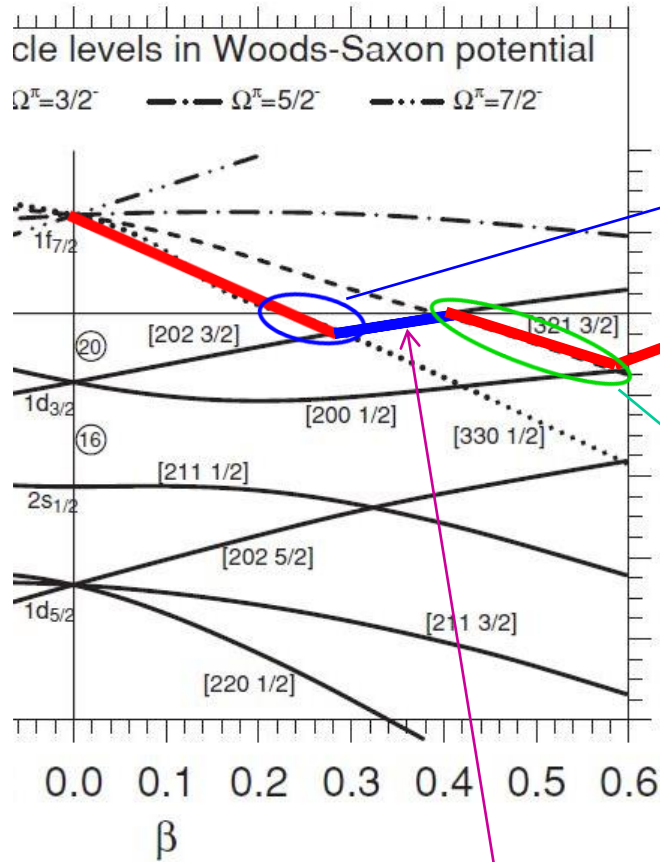


$l = 1$ component is also enhanced when weakly bound (but, always less than 100%)

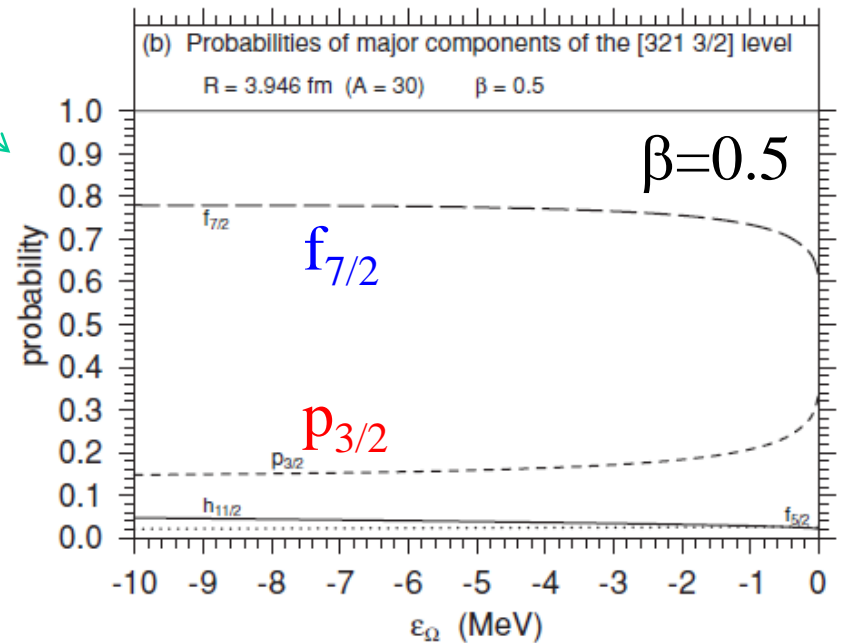
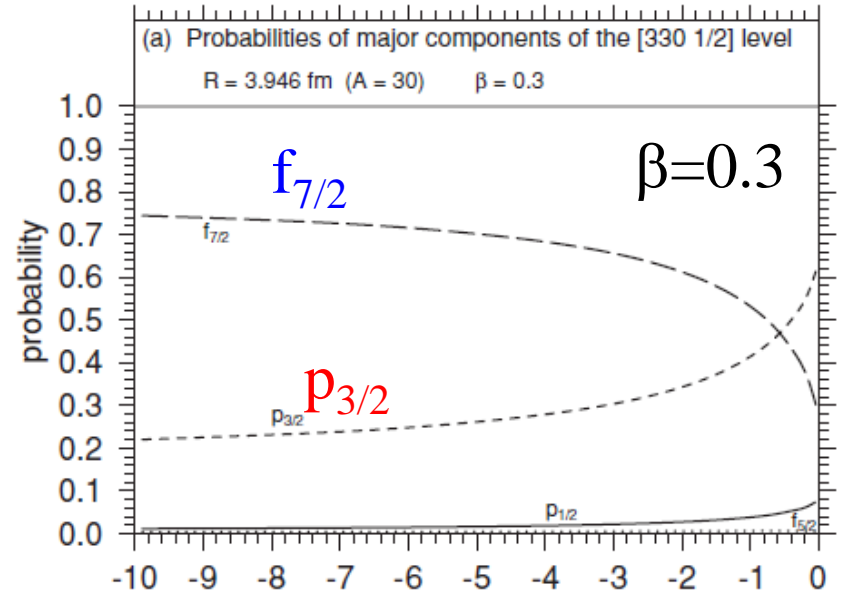


a possibility of deformed halo nucleus: ^{31}Ne

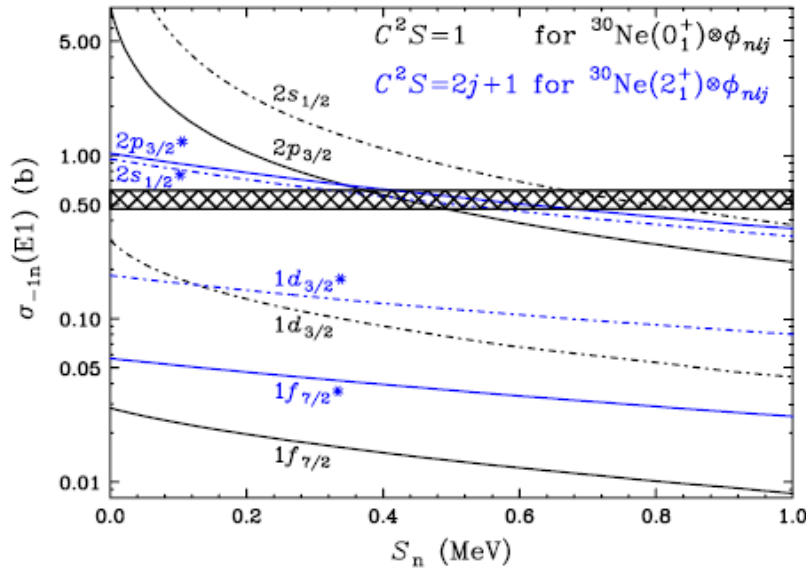
Nilsson model analysis [I. Hamamoto, PRC81('10)021304(R)]



non-halo
($\Omega^\pi = 3/2^+$)

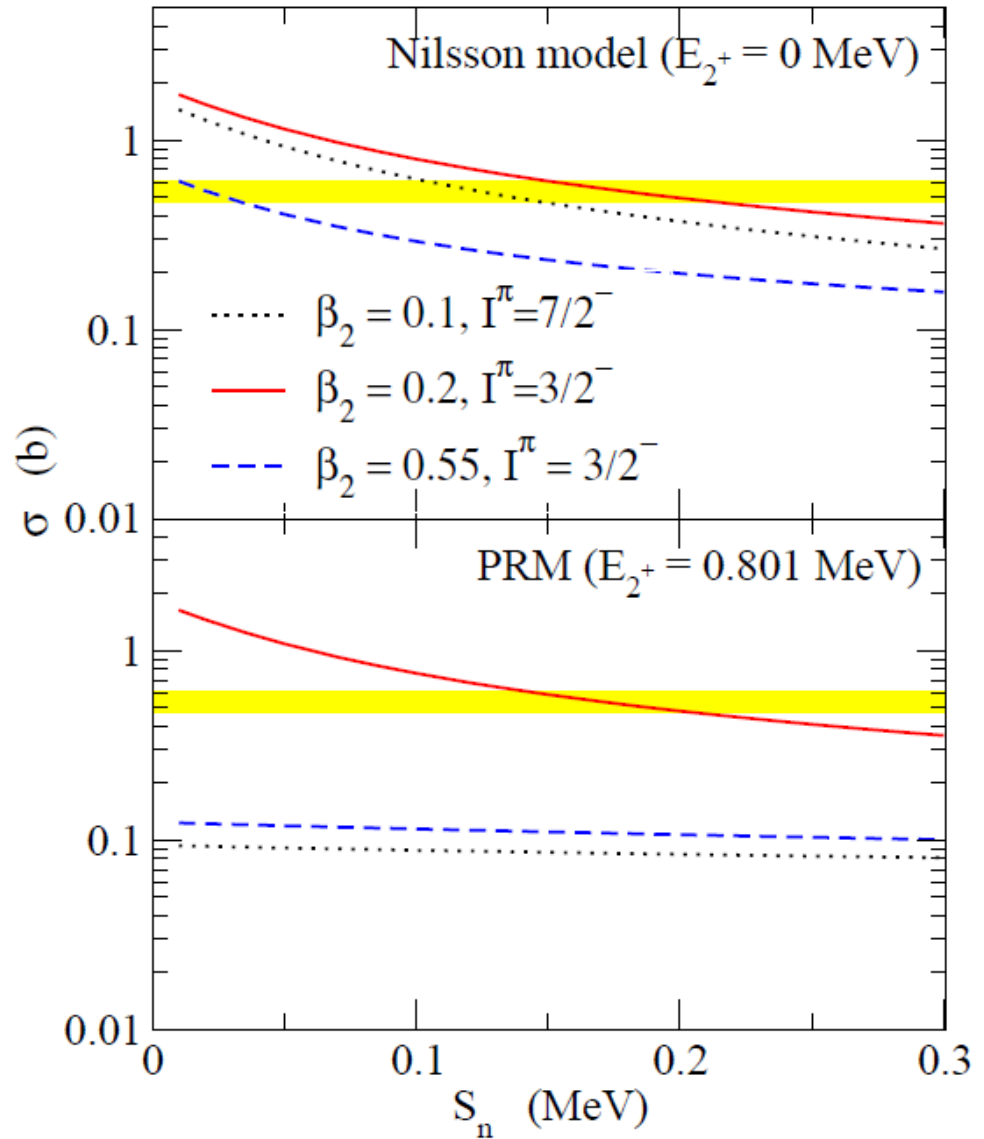


^{31}Ne



Large Coulomb breakup
cross section

T. Nakamura et al.,
PRL103('09)262501



Y. Urata, K.Hagino, and H. Sagawa,
PRC83('11)041303(R)

Observation of a p -Wave One-Neutron Halo Configuration in ^{37}Mg

N. Kobayashi,^{1,*} T. Nakamura,¹ Y. Kondo,¹ J. A. Tostevin,^{2,1} Y. Utsuno,³ N. Aoi,^{4,†} H. Baba,⁴ R. Barthelemy,⁵ M. A. Famiano,⁵ N. Fukuda,⁴ N. Inabe,⁴ M. Ishihara,⁴ R. Kanungo,⁶ S. Kim,⁷ T. Kubo,⁴ G. S. Lee,¹ H. S. Lee,⁷ M. Matsushita,^{4,‡} T. Motobayashi,⁴ T. Ohnishi,⁴ N. A. Orr,⁸ H. Otsu,⁴ T. Otsuka,⁹ T. Sako,¹ H. Sakurai,⁴ Y. Satou,⁷ T. Sumikama,^{10,§} H. Takeda,⁴ S. Takeuchi,⁴ R. Tanaka,¹ Y. Togano,^{4,¶} and K. Yoneda⁴

¹*Department of Physics, Tokyo Institute of Technology, 2-12-1 O-Okayama, Meguro, Tokyo 152-8551, Japan*

²*Department of Physics, Faculty of Engineering and Physical Sciences, University of Surrey, Guildford, Surrey GU2 7XH, United Kingdom*

³*Japan Atomic Energy Agency, Tokai, Ibaraki 319-1195, Japan*

⁴*RIKEN Nishina Center, Hirosawa 2-1, Wako, Saitama 351-0198, Japan*

⁵*Department of Physics, Western Michigan University, Kalamazoo, Michigan 49008, USA*

⁶*Astronomy and Physics Department, Saint Mary's University, Halifax, Nova Scotia B3 H 3C3, Canada*

⁷*Department of Physics and Astronomy, Seoul National University, Seoul 151-742, Korea*

⁸*LPC-Caen, ENSICAEN, IN2P3-CNRS, Université de Caen, 14050 Caen Cedex, France*

⁹*CNS, University of Tokyo, RIKEN Campus, Wako, Saitama 351-0198, Japan*

¹⁰*Department of Physics, Tokyo University of Science, Chiba 278-8510, Japan*

(Received 13 March 2014; published 18 June 2014)